ÇUKUROVA UNIVERSITY
INSTITUTE OF NATURAL AND APPLIED SCIENCES

MSc THESIS

Mehmet KANAL

A NEW ORTHOGONAL SCALING – WAVELET FUNCTION PAIR BASED ON EXCITATORY POSTSYNAPTIC POTENTIAL FUNCTION

DEPARTMENT OF ELECTRICAL AND ELECTRONICS ENGINEERING

ADANA, 2006

ÇUKUROVA ÜNİVERSİTESİ

FEN BİLİMLERİ ENSTİTÜSÜ

A NEW ORTHOGONAL SCALING – WAVELET FUNCTION PAIR BASED ON EXCITATORY POSTSYNAPTIC POTENTIAL FUNCTION

Mehmet KANAL

YÜKSEK LİSANS TEZİ

ELEKTRİK – ELEKTRONİK MÜHENDİSLİĞİ ANABİLİM DALI

Bu tez 20/09/ 2006 Tarihinde Aşağıdaki Jüri Üyeleri Tarafından Oy Birliği / Oy Çokluğu ile Kabul Edilmiştir.

İmza : ……………………..	İmza : ……………………..	İmza : ……………………….
Yard. Doç. Dr. Sami ARICA	Prof. Dr. Mehmet TÜMAY	Yard. Doç. Dr. Turgay İBRİKÇİ
DANIŞMAN	ÜYE	ÜYE

Bu Tez Enstitümüz Elektrik – Elektronik Mühendisliği Anabilim Dalında Hazırlanmıştır.

Kod No : **Prof. Dr. Aziz ERTUNÇ**

Enstitü Müdürü

ÖZ

YÜKSEK LİSANS TEZİ

A NEW ORTHOGONAL SCALING – WAVELET FUNCTION PAIR BASED ON EXCITATORY POSTSYNAPTIC POTENTIAL FUNCTION

Mehmet KANAL

ÇUKUROVA ÜNİVERSİTESİ
FEN BİLİMLERİ ENSTİTÜSÜ
ELEKTRİK – ELEKTRONİK ANABİLİM DALI

Danışman Yard. Doç. Dr. Sami ARICA
Yıl 2006, Sayfa 72
Jüri Yard. Doç. Dr. Sami ARICA
Prof. Dr. Mehmet TÜMAY
Yard. Doç. Dr. Turgay İBRİKÇİ

Beyin insan vücudunun en karmaşık organıdır. Beyinle ilgili birçok bilinmeyen vardır. Elektroansefalografi (EEG), sinir hücrelerinin içinde oluşturulan akımın sebep olduğu beynin elektriksel aktivitelerini ölçen bir yöntemdir. Bir EEG sinyali excitatory ve inhibitory postsynaptic potansiyellerinin (EPSP ve IPSP) bir seri açılımı olarak düşünülebilir. Sentez temel fonksiyonları (EPSP ve IPSP) ortogonal olmadığı için bu açılım ortogonal değildir. Bu çalışmanın amacı EPSP işaretinden yeni bir ortogonal dalgacık elde etmektir.

Anahtar Kelimeler: Elektroansefalografi, EPSP, Çoklu Çözünürlük Analizi, Dalgacık Dönüşümü,

ABSTRACT

MSc THESIS

A NEW ORTHOGONAL SCALING – WAVELET FUNCTION PAIR BASED ON EXCITATORY POSTSYNAPTIC POTENTIAL FUNCTION

Mehmet KANAL

DEPARTMENT OF ELECTRICAL AND ELECTRONICS ENGINEERING
INSTITUTE OF NATURAL AND APPLIED SCIENCES
UNIVERSITY OF ÇUKUROVA

Supervisor Assist. Prof. Dr. Sami ARICA
Year 2006, Pages 72
Jury Assist. Prof. Dr. Sami ARICA
Prof. Dr. Mehmet TÜMAY
Assist. Prof. Dr. Turgay İBRİKÇİ

Brain is the most complex organ of human body. There are many unknowns about brain. Electroencephalography (EEG) is a technique for measuring the electrical activity of the brain that is caused by the current generated within neurons. An EEG signal can be considered as a series of excitatory and inhibitory postsynaptic potentials (EPSP's and IPSP's). This expansion is not orthogonal since the synthesis basis functions (EPSP's and IPSP's) are not orthogonal. The aim of this study is to generate a new orthogonal wavelet from EPSP.

Key Words: Electroencephalography, EPSP, Multiresolution Analysis, Wavelet Transform

ACKNOWLEDGEMENT

First of all I would like to express my appreciation to my supervisor Assist. Prof. Dr. Sami ARICA for all of his supports, guidance, suggestions, patience and encouragement on initiating, improving and completing this study.

I would like to extend my heartfelt appreciation to my parents for their constant love, moral and support.

CONTENTS **Page**

FIGURE LIST

1. INTRODUCTION

A function or signal can be viewed as composed of a smooth background and fluctuations or details on top of it. The distinction between the smooth part and the details is determined by the resolution, that is, by the scale below which the details of a signal cannot be discerned. At a given resolution, a signal is approximated by ignoring all fluctuations below that scale. We can imagine progressively increasing the resolution; at each stage of the increase in resolution finer details are added to the coarser description, providing a successively better approximation to the signal. Eventually when the resolution goes to infinity, we recover the exact signal. The above intuitive description can be made more precise as follows. We label the resolution level by an integer j. The scale associated with the level $j=0$ is set to, say, unity and that with the level j is $1/2^j$. Let us consider a function $f(t)$. At resolution level j it is approximated by $f_j(t)$. At the next level of resolution $j+1$, the details at that level denoted by $d_j(t)$ are included and we have the approximation to $f(t)$ at the new resolution level, $f_{j+1}(t) = f_j(t) + d_j(t)$. The original function $f(t)$ is recovered when we let the resolution go to infinity

$$f(t) = f_j(t) + \sum_{k=j}^{\infty} d_k(t)$$

The word multiresolution refers to the simultaneous presence of different resolutions. The above equation represents one way of decomposing the function $f(t)$ into a smooth part plus details. Similarly, we can view the space of functions that are square integrable, $L^2(R)$, as composed of a sequence of subspaces $\{W_k\}$ and V_j, such that the approximation of $f(t)$ at resolution j, $f_j(t)$, is in V_j and the details $d_k(t)$ are in W_k . This brings us to the subject of this section, multiresolution analysis.

2. MULTIRESOLUTION ANALYSIS

We discuss the requirements imposed on a multiresolution analysis qualitatively. Consider the space of square-integrable functions. We define a sequence of resolutions labeled by the integers such that all details of the signal on scales smaller than 2^{-j} are suppressed at resolution j. We denote the subspace of functions that contain signal information down to scale 2^{-j} by V_j. The multiresolution analysis involves a decomposition of the function space into a sequence of subspaces V_j (Mallat, 1989). The first requirement is that the subspace V_j be contained in all the higher subspaces. This is clearly reasonable. If we denote the approximation to $f(t)$ at level j by $f_j(t)$, then $f_j(t) \in V_j$. Since information at resolution level j is necessarily included in the information at a higher resolution, V_j must be contained in V_{j+1}, that is, mathematically, $V_j \subset V_{j+1}$ for all j. The difference between $f_{j+1}(t)$ and $f_j(t)$ is the additional information about details at scale $2^{-(j+1)}$ which we denoted earlier by $d_j(t) = f_{j+1}(t) - f_j(t)$. So we have

$$f_{j+1}(t) = f_j(t) + d_j(t)$$

We can decompose our subspaces accordingly, and write

$$V_{j+1} = V_j \oplus W_j$$

Where W_j is called the detail space at resolution level j and is orthogonal to V_j. This means that the inner product between any element in W_j and any element in V_j vanishes. (We call two spaces that satisfy this property orthogonal and use $V_j \perp W_j$ to denote V_j is orthogonal to W_j.) We can continue the decomposition of the V space and obtain

$$V_{j+1} = W_j \oplus V_j = W_j \oplus W_{j-1} \oplus V_{j-1} = ... = W_j \oplus W_{j-1} \oplus W_{j-2} \oplus ... \oplus W_{j-J} \oplus V_{j-J}$$

So the approximation space at resolution j, V_j, can be written as a sum of subspaces. It is easy to see that these subspaces are mutually orthogonal. Since $V_j \perp W_j$, W_j should be orthogonal to any subspace of V_j. Because both V_{j^t} and W_{j^t} are contained in V_j for $j^t<j$, we have $W_j \perp V_{j^t}$ for $j > j^t$, and $W_j \perp W_{j^t}$ when $j \neq j^t$. This is to say any two detail spaces at different resolutions are orthogonal, and the detail space W_j is orthogonal to an approximation space V_{j^t} only when the detail space has higher resolution.

The second requirement for multiresolution analysis is that all square integrable functions be included at the finest resolution and only the zero function at the coarsest level. As the resolution gets coarser and coarser, more and more details are removed, and in the limit $j \to -\infty$, only a constant function survives and since it has to be square integrable, it can only be the zero function. Therefore, we demand that $\lim_{j\to-\infty} V_j = \{0\}$. On the other hand, when we increase the resolution, more details are included and as the resolution goes to infinity, we should recover, crudely speaking, the entire initial space $L^2(R)$, that is, $\lim_{j\to\infty} V_j = L^2(R)$.

The third condition is the key requirement of scale or dilation invariance. It says that all the spaces $\{V_j\}$ are scaled versions of the central space V_0. If $f(t)$ is in V_j, that is, $f(t)$ contains no details or fluctuations at scales smaller than $1/2^j$, then $f(2t)$ is a function obtained by squeezing $f(t)$ by a factor of 2 and contains no details at scales smaller than $1/2^{j+1}$. Therefore, $f(2t)$ is in V_{j+1}.

The fourth condition is the requirement of translation or shift invariance of the space V_j. If $f(t) \in V_0$, so do its translates by integers, $\{f(t-k)\}$. Given this, one can show that all the subspaces $\{V_j\}$ are also shift-invariant. The third and fourth requirements of dilation and translation invariance yield the result that if $f(t) \in V_0$, $f(2^j t - k) \in V_j$.

The final requirement is that there exists a function ϕ such that its translates form an orthonormal basis for V_0. Using the scale invariance condition, we see that $\{\phi(2t-k)\}$ is an orthogonal basis for V_1. Similarly, if we define

$\phi_{jk}(t) = 2^{j/2}\phi(2^j t - k)$, then $\{\phi_{jk}(t)\}$ forms an orthonormal basis for V_j. The function ϕ, which generates the basis functions for all the spaces *$\{V_j\}$*, is called the *scaling function* of the multiresolution analysis.

A multiresolution analysis of $L^2(R)$ is a nested sequence of subspaces $\{V_j\}_{j\in Z}$ (Z is the set of integers) such that

(i) $\ldots \subset V_{-1} \subset V_0 \subset V_1 \subset \ldots \subset L^2(R)$

(ii) $\bigcap_j V_j = \{0\}, \overline{\bigcup_j V_j} = L^2(R)$

(iii) $f(t) \in V_j \Leftrightarrow f(2t) \in V_{j+1}$

(iv) $f(t) \in V_0 \Rightarrow f(t-k) \in V_0$

(v) There exists a function $\phi(t)$, called the scaling function, such that $\{\phi(t-k)\}$ is an orthonormal basis of (Mallat, 1989).

2.1. Approximation Spaces, Scaling Function, and The Dilation Equation

From the definition of a multiresolution analysis we know that the subspaces *$\{V_j\}$* form a nested sequence that provides successively better approximations to L^2. The scaling function ϕ generates all the basis functions $\{\phi_{jk}(t)\}$ for each space V_j, where $\phi_{jk}(t) = 2^{j/2}\phi(2^j t - k)$.

Since $V_0 \subset V_1$, any function in V_0 can be expanded in terms of the basis functions of V_1. In particular, the scaling function $\phi \in V_0$ can be expanded in terms $\{\phi_{1k}(t)\}$:

$$\phi(t) = \sum_k h_k \phi_{1k}(t) = \sqrt{2}\sum_k h_k \phi(2t-k) \tag{2.1}$$

This is called the *dilation equation*. This equation relates the scaling function at two successive scales, t and $2t$, and, hence, it is also referred to as the *two-scale equation* or *refinement equation*. Using the fact that $\{\phi_{1k}(t)\}$ are orthonormal, the coefficients *{h}* can be obtained by computing the inner product (assuming ϕ is real):

$$h_k = \langle \phi_{1k}, \phi \rangle = \int_{-\infty}^{\infty} \phi(t)\phi(2t-k)dt \tag{2.2}$$

We can derive some properties of the coefficients $\{h_k\}$ immediately from the dilation equation. Integrating both sides of (2.1), we obtain (note that normalization gives $\int_{-\infty}^{\infty} \phi(t)dt = 1$)

$$\sum_k h_k = \sqrt{2}\,.$$

On the other hand, if we multiply both sides of (2.1) by $\phi(t-l)$ and integrate, we get

$$\int_{-\infty}^{\infty} \phi(t)\phi(t-l)dt = \sum_k \sum_{k'} h_k h_{k'} 2\int_{-\infty}^{\infty} \phi(2t-k')\phi(2t-2l-k)dt = \sum_k h_k h_{k+2l}\,.$$

Using the orthogonality of $\{\phi(t-k)\}$ we have $\sum_k h_k h_{k+2l} = \delta_{0l}$ or

$$\sum_k h_k^2 = 1 \quad \text{and} \quad \sum_k h_k h_{k+2l} = 0, \quad l \neq 0\,.$$

2.2. Detail Spaces, Mother Wavelet, and the Wavelet Equation

Now we examine the spaces $\{W_j\}$. These are detail spaces and they are orthogonal to each other. The detail space W_j has an orthonormal basis $\{\psi_{jk}(t)\}_k$, where $\psi_{jk}(t) \equiv 2^{j/2}\psi(2^j t - k)$. So L^2 has an orthonormal basis $\{\psi_{jk}(t)\}_{jk}$ called the wavelet basis. Each wavelet $\psi_{jk}(t)$ is generated from a single function $\psi(t)$ by translation and dilation. The function $\psi(t)$ that generates all the basis functions of the W space is referred to as the *mother wavelet* or the *basic wavelet*.

Since $\{\psi(t-k)\}$ is in W_0 and $W_0 \subset V_1$, $\psi(t)$ can be written as a superposition of the basis functions for V_1 , $\{\phi_{1k}\}$. In particular, we have

$$\psi(t) = \sum_k g_k \phi_{1k}(t) = \sqrt{2} \sum_k g_k \phi(2t-k) . \tag{2.3}$$

This is called the *wavelet equation*. Note the similarity between this equation and the dilation equation. This is an equation relating the mother wavelet to the scaling function at the next finer scale. Again, using the fact that $\{\phi_{1k}(t)\}$ are orthonormal, the coefficients $\{g_k\}$ can be obtained by computing the inner product:

$$g_k = \langle \phi_{1k}, \psi \rangle = \sqrt{2} \int_{-\infty}^{\infty} \psi(t) \phi(2t-k) dt . \tag{2.4}$$

From the requirement that $\int_{-\infty}^{\infty} \psi(t) dt = 0$, we get $\sum_k g_k = 0$.

2.3. A View from the Frequency Domain

All the above relations can be expressed in the frequency domain or Fourier space. We define the Fourier transform of the scaling function $\hat{\phi}(w)$ by

$$\hat{\phi}(w) = \int_{-\infty}^{\infty} \phi(t) e^{-iwt} dt .$$

Multiplying both sides of the dilation equation by e^{-iwt} and integrating, we have

$$\hat{\phi}(w) = \int_{-\infty}^{\infty} \phi(t) e^{-iwt} dt = \sum_k \sqrt{2} h_k \int_{-\infty}^{\infty} \phi(2t-k) e^{-iwt} dt$$

$$= \left(\sum_k \frac{h_k}{\sqrt{2}} e^{-ikw/2} \right) \int_{-\infty}^{\infty} \phi(2t-k) e^{-i(2t-k)w/2} d(2t) = \left(\sum_k \frac{h_k}{\sqrt{2}} e^{-ikw/2} \right) \hat{\phi}\left(\frac{w}{2} \right).$$

Defining

$$H(w) = \sum_k \frac{h_k}{\sqrt{2}} e^{-ikw},$$

the dilation equation in Fourier space assumes the form

$$\hat{\phi}(w) = H\left(\frac{w}{2}\right)\hat{\phi}\left(\frac{w}{2}\right). \tag{2.5}$$

Similarly, let the Fourier transform of the mother wavelet be $\hat{\psi}(w) = \int_{-\infty}^{\infty} \psi(t) e^{-iwt} dt$ and

$$G(w) = \sum_k \frac{g_k}{2} e^{-ikw} \quad ,$$

the wavelet equation in Fourier space is

$$\hat{\psi}(w) = G\left(\frac{w}{2}\right)\hat{\phi}\left(\frac{w}{2}\right). \tag{2.6}$$

2.4. Orthogonality Conditions in the Frequency Domain

If $\phi(t)$ is orthonormal to its translates $\{\phi(t-k)\}$, we have

$$\delta_{k,0} = \int_{-\infty}^{\infty} \phi(t)\overline{\phi(t-k)}dt = \frac{1}{2\pi}\int_{-\infty}^{\infty} \hat{\phi}(w)\overline{\hat{\phi}(w)}e^{iwk}dw = \frac{1}{2\pi}\int_0^{2\pi} \sum_{l=-\infty}^{\infty} \left|\hat{\phi}(w+2\pi l)\right|^2 e^{iwk}dw.$$

But the last expression is exactly the coefficient a_k in the Fourier series expansion of the 2π periodic function $A(w) \equiv \sum_{l=-\infty}^{\infty} \left|\hat{\phi}(w+2\pi l)\right|^2$. In other words,

$$\sum_{l=-\infty}^{\infty} \left|\hat{\phi}(w+2\pi l)\right|^2 = \sum_k a_k e^{-ikw} = 1 .$$

So the orthonormality of $\{\phi(t-k)\}$ can be expressed in the frequency domain as

$$\sum_{l=-\infty}^{\infty} \left|\hat{\phi}(w+2\pi l)\right|^2 = 1 . \tag{2.7}$$

If a set of basis functions $\{\phi(t-k)\}$ are not orthonormal, we can orthogonalize them easily in Fourier space. All we need to do is to divide $\hat{\phi}(w)$ by the square root of $\sum_{l=-\infty}^{\infty} \left|\hat{\phi}(w+2\pi l)\right|^2$,

$$\hat{\phi}_{orth}(w) = \frac{\hat{\phi}(w)}{\sqrt{\sum_{l=-\infty}^{\infty} \left|\hat{\phi}(w+2\pi l)\right|^2}} \tag{2.8}$$

and

$$\sum_{k=-\infty}^{\infty} \left|\hat{\phi}_{orth}(w+2\pi k)\right|^2 = \sum_k \left| \frac{\hat{\phi}(w+2\pi k)}{\sqrt{\sum_{l=-\infty}^{\infty} \left|\hat{\phi}(w+2\pi l)\right|^2}} \right|^2 = 1 .$$

$\hat{\phi}_{orth}(w)$ satisfies the orthonormality condition (2.7), so $\{\hat{\phi}_{orth}(t-k)\}$ are orthonormal. Using the dilation equation (2.5), we can also rewrite the orthonormality condition (2.7) as a condition on *H(w)*:

$$\sum_{l=-\infty}^{\infty} \left|\hat{\phi}(w+2\pi l)\right|^2 = \sum_{l=-\infty}^{\infty} \left|H\left(\frac{w+2\pi l}{2}\right)\right|^2 \left|\hat{\phi}\left(\frac{w+2\pi l}{2}\right)\right|^2 = \sum_{l=-\infty}^{\infty} \left|H(w'+\pi l)\right|^2 \left|\hat{\phi}(w'+\pi l)\right|^2 = 1 .$$

Since the above equation is true for all $w' = w/2$, we can simply replace it by *w*. Separating the sum into even (*l=2k*) and odd (*l=2k+1*) terms, we have

$$\sum_{k=-\infty}^{\infty} |H(w+2k\pi)|^2 \left|\hat{\phi}(w+2k\pi)\right|^2 + \sum_{k=-\infty}^{\infty} |H(w+(2k+1)\pi)|^2 \left|\hat{\phi}(w+(2k+1)\pi)\right|^2 = 1\,.$$

Again, using the fact that *H(w)*is 2π periodic, the above equation reduces to

$$|H(w)|^2 \sum_{k=-\infty}^{\infty} \left|\hat{\phi}(w+2k\pi)\right|^2 + |H(w+2k\pi)|^2 \sum_{k=-\infty}^{\infty} \left|\hat{\phi}((w+\pi)+2k\pi)\right|^2 = 1.$$

This gives

$$|H(w)|^2 + |H(w+\pi)|^2 = 1\,, \tag{2.9}$$

the condition on *{h_k}*for $\{\phi(t-k)\}$ to be orthogonal.

The orthogonality conditions for the wavelets in the frequency domain can be derived in a completely parallel fashion. For example, for $\{\psi(t-k)\}$ to be orthonormal, we must have

$$\sum_{l=-\infty}^{\infty} |\hat{\psi}(w+2\pi l)|^2 = 1\,,$$

or

$$|G(w)|^2 + |G(w+\pi)|^2 = 1\,.$$

We can also derive the condition in frequency space that $\{\psi(t-k)\}$ and $\{\phi(t-k)\}$ are orthogonal,

$$0=\int_{-\infty}^{\infty}\phi(t)\overline{\psi(t-k)}dt=\frac{1}{2\pi}\int_{-\infty}^{\infty}\hat{\phi}(w)\overline{\hat{\psi}(w)}e^{iwk}dw=\frac{1}{2\pi}\int_{0}^{2\pi}\sum_{l=-\infty}^{\infty}\hat{\phi}(w+2\pi l)\overline{\hat{\psi}(w+2\pi l)}e^{iwk}dw$$

Since the Fourier coefficients of the function $\sum_{l=-\infty}^{\infty}\hat{\phi}(w+2\pi l)\overline{\hat{\psi}(w+2\pi l)}$ are identically zero, we conclude,

$$\sum_{l=-\infty}^{\infty}\hat{\phi}(w+2\pi l)\overline{\hat{\psi}(w+2\pi l)}=0\,.$$

Similarly, using the dilation equation (2.5) and the wavelet equation (2.6) to rewrite the above equation, we have

$$H(w)\overline{G(w)}+H(w+\pi)\overline{G(w+\pi)}=0\,.$$

This is the condition that has to be satisfied if $\{\psi(t-k)\}$ and $\{\phi(t-k)\}$ are orthogonal. This equation relates the coefficients appearing in the wavelet equation *$\{g_k\}$* to those appearing in the dilation equation *$\{h_k\}$* (Zhou, Do and Kovaccevic, 2003). To find the explicit relationship between the two sets of coefficients we need to solve the equation. It is obvious that the above equation is satisfied if *$G(w)$* is chosen to be

$$G(w)=\lambda(w)\overline{H(w+\pi)}\,,$$

where $\lambda(w)=-\lambda(w+\pi)$ is a 2π periodic function and $|\lambda(w)|^2=1$. The orthogonality conditions do not specify G or the wavelet uniquely, we have the freedom of choosing the 2π periodic function of unit modulus λ. Here we will follow the usual convention of choosing $\lambda(w)=-e^{-iw}$ and stick to it, but it should be borne in mind that other valid choices are possible.

Thus, finally we have determined the relationship between the coefficients in the dilation equation and those in the wavelet equation. They are related through $G(w) = -e^{-iw} H(w+\pi)$

Or, writing out *H(w)* explicitly,

$$G(w) = -e^{-iw} \sum_k \frac{h_k}{\sqrt{2}} e^{i(w+\pi)k} = \sum_k \frac{h_k}{\sqrt{2}} (-1)^{1-k} e^{-iw(1-k)} = \sum_n \frac{(-1)^n h_{1-n}}{\sqrt{2}} e^{-iwn} \ .$$

We immediately identify

$$g_n = (-1)^n h_{1-n} \ . \tag{2.10}$$

So we see that once the scaling function ϕ is known, the coefficients $\{h_n\}$ are obtained by calculating the inner products of ϕ and ϕ_{1k}. In turn, the coefficients of $\{g_n\}$ are known from (2.10) and, using the wavelet equation, we get the wavelet. On the other hand, if we know the coefficients $\{h_n\}$, we can find the scaling function by solving the dilation equation.

3. WAVELETS TRANSFORM

Wavelet transform is in a way similar to Fourier series. In Fourier series, a signal is represented by a sum of infinite frequency sinusoids. In wavelet transform, a signal is represented by a sum of scaled and shifted wavelets. Wavelets are not sinusoids. However, the scaling factor is related to the frequency (Fomitchev, 1994). The bigger the scaling factor is, the narrower the wavelet is. Narrow wavelets are comparable to high-frequency sinusoids and wide wavelets are comparable to low-frequency sinusoids. The wavelet transform is better than Fourier series in a sense that it can grab better the locality of a signal. Fourier series will work well only when a signal is stationary for a long period of time. Because of this nature, wavelet transform is getting more attention recently. We can classify wavelets into two classes: (a) orthogonal and (b) biorthogonal. Based on the application, either of them can be used.

3.1. Orthogonal Wavelets

We have seen in the earlier sections that wavelets provide special kinds of bases in function space. Their novelty lies partly in the fact that all the functions of the basis $\{\psi_{jk}(t)\}$ are derived from a single function $\psi(t)$, called the basic wavelet or mother wavelet, by translations and dilations:

$$\psi_{jk}(t) = 2^{j/2}\psi(2^j t - k).$$

There are essentially two approaches to finding the scaling function $\phi(t)$. The first starts from a multiresolution analysis. Usually, there exists a known, nonorthogonal basis for V_0 , and all we need to do is to use the orthogonalization procedure to obtain the scaling function that generates the orthogonal basis. The second approach is to find the coefficients $\{h_n\}$ in the dilation equation (2.1) that obey appropriate conditions, and the scaling function $\phi(t)$ can then be constructed from the dilation equation.

In this section we illustrate the first approach to finding a scaling function $\phi(t)$ and, in turn, the associated wavelet $\psi(t)$. The scaling functions are simply the orthogonalized *B-spline* functions. Yet another related approach to finding a scaling function is to specify the appropriate scaling function in frequency space

3.1.1. Spline Functions

We consider the space S_n of polynomial spline functions of order n with knots at integers defined as follows: S_n is a collection of functions $f(t)$ that satisfy the following two properties:

(i) in each interval $[k, k+1)$ (k integer), $f(t)$ is a polynomial of degree not exceeding n, and

(ii) for $n>0$, $f(t)$ is smooth in that the first $(n-1)$ derivatives are continuous.

The functions $f(t)$ so defined are often called *cardinal spline functions*. However, for simplicity we will refer to them simply as spline functions or polynomial splines. For example, when $n=0$, S_0 consists of piecewise constant functions with possible discontinuities at the integers. The box function translates form a basis for S_0, since any piecewise constant function in S_0 can obviously be written as a superposition of these basis functions. We call the box function a B-spline of order zero, where the B stands for basis, and denote it by $\beta_0(t)$. That is, $\beta_0(t)=1$ if $0 \le t < 1$ and $\beta_0(t)=0$ otherwise, and $\{\beta_0(t-k)\}$ is a basis for S_0.

For $n=1$, S_1, the space of polynomial splines of order 1, consists of piecewise linear functions with possible discontinuities in the first derivative at the integers. This means that the derivative of any spline function of order 1 is a spline function of order zero and suggests that the basis functions for S_1 can be obtained by integrating those of S_0. In fact, one choice for the B-spline of order 1 can be written in the form

$$\int_0^1 \beta_0(t-x)dx = \int_{-\infty}^{\infty} \beta_0(x)\beta_0(t-x)dx\,,$$

that is, a convolution of a B-spline of order zero with itself. Since $\beta_0(t-x)$ is nonzero only when t-x is within [0, 1), the integral vanishes except when $t-1 < x \le t$. That is,

$$\int_{-\infty}^{\infty} \beta_0(x)\beta_0(t-x)dx = \int_0^1 \beta_0(t-x)dx = \int_{\max(0\,j-1)}^{\min(1\,j)} dt = \begin{cases} t & if\ 0 \le t \le 1 \\ 2-t & if\ 1 \le t \le 2 \\ 0 & otherwise \end{cases}$$

This is the hat function defined on the interval [0, 2]. We will choose the hat function defined on the interval [-1, 1] as our B-spline function of order one $\beta_1(t)$, that is, $\beta_1(t)$ is obtained by translating the above function by unity:

$$\beta_1(t) = \begin{cases} 1-|t|, & -1 \le t \le 1 \\ 0 & otherwise \end{cases} \tag{3.1}$$

and $\{\beta_1(t-k)\}$ form a basis for S_1.

The higher-order B-spline functions can be obtained similarly using convolutions. In general, the n^{th} order B-spline $\beta_n(t)$ is obtained from an n-fold convolution of $\beta_0(t)$. It is a polynomial of degree n with support of length $n+1$. Here in our discussion we choose its support to be [$-(n+1)/2, (n+1)/2$] for odd n and [$-n/2, n/2+1$] for even n, so that $\beta_n(t)$ is symmetric about $t=0$ for n odd and about $t=1/2$ for n even. If we define $[t]_+ = max(0,t)$ and $[t]_+^n = ([t]_+)^n$, an explicit formula for B-spline of order $n>0$ is

$$\beta_n(t) = \begin{cases} \dfrac{1}{n!}\displaystyle\sum_{j=0}^{n+1}(-1)^j \binom{n+1}{j}\left[t+n/2-j\right]_+^n & for\ n\ even \\ \dfrac{1}{n!}\displaystyle\sum_{j=0}^{n+1}(-1)^j \binom{n+1}{j}\left[t+(n+1)/2-j\right]_+^n & for\ n\ odd \end{cases} \tag{3.2}$$

and $\{\beta_n(t-k)\}$ is a basis for S_n, the space of polynomial splines of order *n*. Here we display *B*-spline of order 4.

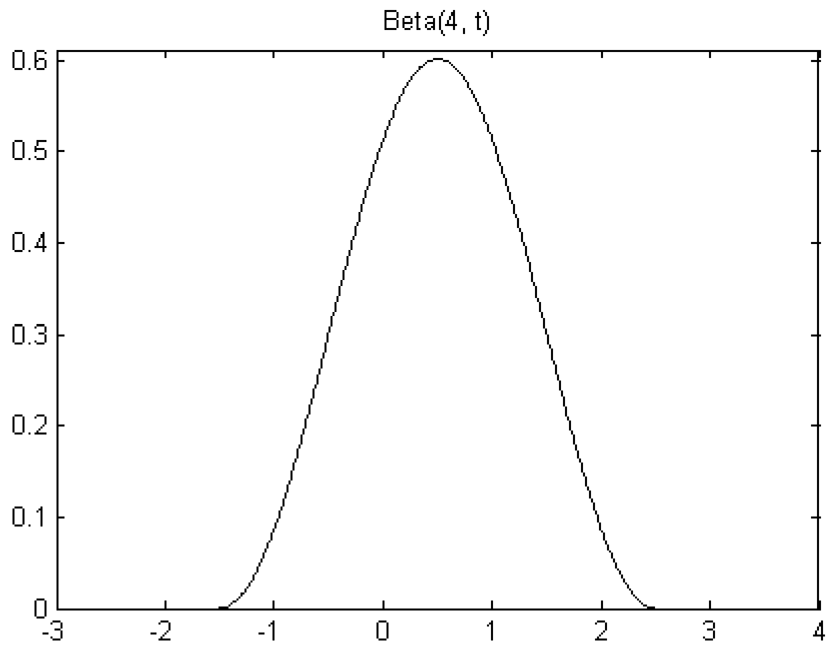

Figure 3.1. B-Spline function of order 4

The basis functions $\{\beta_n(t-k)\}$ are not orthogonal except in the case of *n=0*. This can be understood from the fact the $\beta_n(t)$ is nonnegative and has support of length *n+1*, and the graphs of $\beta_n(t-1)$ and $\beta_n(t)$ necessarily overlap when $n \neq 0$.

3.1.1.1. Spline Multiresolution Analyses

Starting from the space of spline functions of order *n* ($n \geq 0$), S_n, we can build a multiresolution analysis of $L^2(R)$. Let V_0 be the space containing functions of S_n that are square-integrable. That is, if $f(t) \in V_0$, $f(t) \in L^2$, and *f(t)* is a polynomial of degree not exceeding *n* in each interval [k, k+1) (*k* integer), and its first *n-1* derivatives are continuous with possible discontinuities in higher derivatives occurring only at the integers. The space V_1 is then the space containing square-integrable polynomial functions of degree at most *n* on each half intervals with the first *n-1* derivatives continuous. Therefore, we obviously have $V_0 \subset V_1$. We can show that there is a nested sequence of subspaces of L^2 and conditions (i) to (iv) for $\{V_j\}$ to be a multiresolution analysis are satisfied. Now it remains to be shown that there exists a scaling function ϕ such that $\{\phi(t-k)\}$ forms an orthonormal basis for V_0. In fact, we already have a basis for V_0 , $\{\beta_n(t-k)\}$. All we need to do is to use the orthogonalization trick to make it orthogonal. In addition, since $V_0 \subset V_1$, we can express $\beta_n(t)$ in terms of the basis of V_1, $\{\beta_n(2t-k)\}$. In fact, $\beta_n(t)$ satisfies the following two-scale equation:

$$\beta_n(t) = \begin{cases} \dfrac{1}{2\pi}\displaystyle\sum_{j=0}^{n+1}\binom{n+1}{j}\beta_n(2t+n/2-j) & \textit{for n even} \\ \dfrac{1}{2\pi}\displaystyle\sum_{j=0}^{n+1}\binom{n+1}{j}\beta_n(2t+(n+1)/2-j) & \textit{for n odd} \end{cases} \tag{3.3}$$

For example, for $n=1$ we have

$$\beta_1(t) = \frac{1}{2}[\beta_1(2t+1) + 2\beta_1(2t) + \beta_1(2t-1)]$$

and for $n=2$,

$$\beta_2(t) = \frac{1}{4}[\beta_2(2t+1) + 3\beta_2(2t) + 3\beta_2(2t-1) + \beta_2(2t-2)]$$

The two-scale relation (3.3) can be seen clearly by plotting β_n at scale t and $2t$ together. The following graph show the two-scale relation for $n=2$. The solid line is $\beta_n(t)$ and it is the sum of the dashed curves that are translated versions of $\beta_n(2t)$ multiplied by the appropriate coefficients.

3.1.1.2. Orthogonalization of the *B*-Spline Functions

We now show how we can orthogonalize $\beta_n(t)$ to get an orthogonal scaling function using the formula given in (2.8). Here we will refer to $\beta_n(t)$ as the nonorthogonal scaling function and use $\phi(t)$ to denote the (orthogonal) scaling function. Note that for simplicity we have omitted the subscript *n*, but the *n* dependence of ϕ should be clear. The Fourier transform of the *B*-spline function $\beta_0(t)$ is

$$\hat{\beta}_0(w) = \int_{-\infty}^{\infty} \beta_0(t) e^{-iwt} dt = \int_0^1 e^{-iwt} dt = (1 - e^{-iw})/(iw) = e^{-iw/2} \frac{\sin w/2}{w/2} \tag{3.4}$$

Since the *B*-spline function of order *n*, $\beta_n(t)$, is the convolution of *n+1* zeroth order *B*-splines, its Fourier transform is that of the zeroth order *B*-spline raised to the (n+1)$^{\text{th}}$ power:

$$\hat{\beta}_n(w) = e^{-ikw/2} \left(\frac{\sin w/2}{w/2} \right)^{n+1} \tag{3.5}$$

Depending on where the center of $\beta_n(t)$ is located, the phase factor $e^{-ikw/2}$ assumes different values. $\beta_n(t)$ is symmetric about *t=0* for *n* odd and about *t=1/2* for *n* even. This corresponds to the choice *k=0* if *n* is odd and *k=1* if *n* is even in the above expression.

To orthogonalize $\beta_n(t)$ it is useful to first calculate the quantity *b(w)* which is defined by

$$b(w) \equiv \sum_l \left| \hat{\beta}_n(w + 2\pi l) \right|^2 = (2\sin w/2)^{2(n+1)} \sum_l \frac{1}{(w + 2\pi l)^{2(n+1)}} = (2\sin w/2)^{2(n+1)} \Sigma_{2(n+1)}(w)$$

In the last equality we have introduced the notation

$$\Sigma_n(w) \equiv \sum_l \frac{1}{(w+2\pi l)^n}.$$

It is straightforward to see that

$$\Sigma_n(w) = \frac{(-1)^{n-2}}{(n-1)!}\frac{d^{n-2}}{dw^{n-2}}\Sigma_2(w).$$

Therefore,

$$\Sigma_2(w) = \frac{1}{4\sin^2 w/2}.$$

So, the desired scaling function, that is, the orthogonalized *B*-spline function of order *n*, is, in Fourier space,

$$\hat{\phi}(w) = \frac{\hat{\beta}_n(w)}{\sqrt{(2\sin w/2)^{2(n+1)}\Sigma_{2(n+1)}(w)}} \equiv M(w)\hat{\beta}_n(w) \qquad (3.6)$$

Where $M(w) = 1/\sqrt{b(w)}$ is an even, 2π -periodic function of *w*. To find the scaling function $\phi(t)$, the straightforward procedure is to apply the inverse Fourier transform to $\hat{\phi}(w)$. A simpler way of finding $\phi(t)$ is to find $\{c_k\}$, where

$$M(w) = \sum_k c_k e^{-ikw}$$

is the discrete Fourier transform of $\{c_k\}$, and the scaling function is given by

$$\phi(t) = \sum_k c_k \beta_n(t-k)$$

We see that since *M(w)* is a trigonometric polynomial raised to the negative *1/2* power, its expansion in terms of Fourier series will have infinite number of terms. This in turn shows that, unlike the nonorthogonal scaling function $\beta_n(t)$, the orthogonalized scaling function $\phi(t)$ will not have finite support. This means that in principle we need to calculate infinitely many $\{c_k\}$ in order to get $\phi(t)$. However, in practice, the coefficients $\{c_k\}$ decay exponentially fast with k and we can truncate the series at some k_{max} depending on the required accuracy.

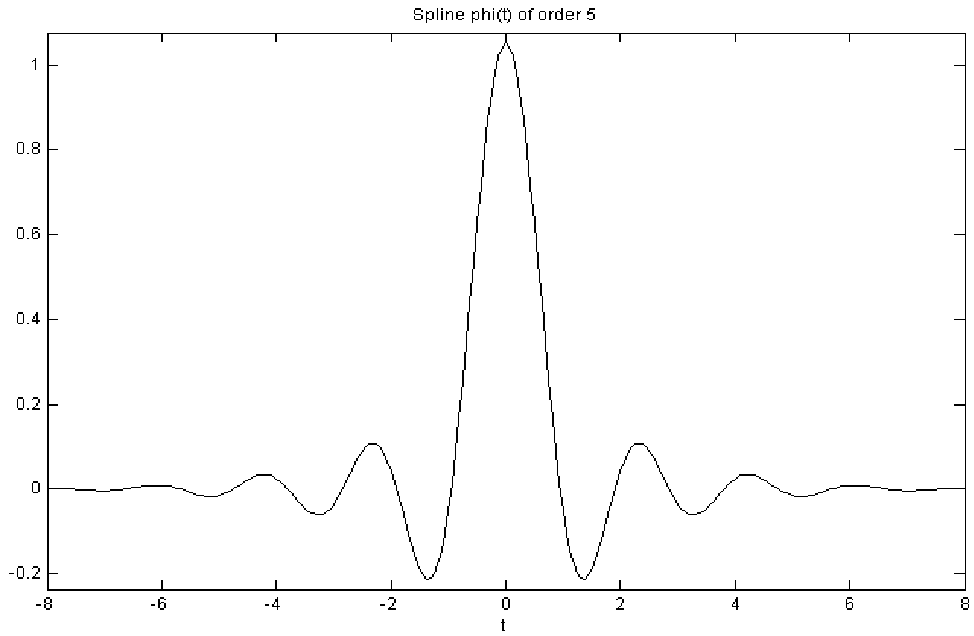

Figure 3.2. Spline phi(t) of order 5

3.1.1.3 Spline Filters and Wavelets

The mother wavelet $\psi(t)$ is obtained from the wavelet equation

$$\psi(t) = \sum_k \sqrt{2} g_k \phi(2t-k) \tag{3.7}$$

where $\phi(t)$ is the scaling function of the multiresolution analysis and the coefficients $\{g_k\}$ are related to $\{h_k\}$through

$$g_k = (-1)^k h_{1-k} .$$

$\{h_k\}$are the coefficients appearing in the dilation equation:

$$\phi(t) = \sum_k \sqrt{2} h_k \phi(2t - k) \ .$$

Therefore, once we know the scaling function, the mother wavelet $\psi(t)$ can be obtained if the coefficients $\{h_k\}$, called filter coefficients, are known. If the support of $\phi(t)$ is infinite, the sums in both the dilation equation and the wavelet equation are infinite. In practice, we only calculate the finite number of the coefficients and truncate the sums at k=k_{max} depending on the accuracy required for a particular application.

We first describe the calculation of the spline filter coefficients. Recall that the dilation equation in Fourier space assumes the form

$$\hat{\phi}(w) = H\left(\frac{w}{2}\right)\hat{\phi}\left(\frac{w}{2}\right),$$

Where $H(w) = \sum_k h_k e^{-ikw} / \sqrt{2}$. Therefore, given $H(w)$, $h_k / \sqrt{2}$ can be computed as the k^{th} Fourier coefficient of $H(w)$. To find the expression for $H(w)$ we employ the two-scale equation satisfied by $\beta_n(t)$. In Fourier space it is

$$\hat{\beta}_n(w) = H_b\left(\frac{w}{2}\right)\hat{\beta}_n\left(\frac{w}{2}\right).$$

Substituting the expression for $\hat{\beta}_n(w)$ given in (2.5), we have

$$H_b(w) = \frac{\hat{\beta}_n(2w)}{\hat{\beta}_n(w)} = \left(\frac{\sin w}{w}\frac{w/2}{\sin w/2}\right)^{n+1} \frac{e^{-iwK}}{e^{-iwK/2}} = \left(\cos\frac{w}{2}\right)^{n+1} e^{-iwK/2} .$$

On the other hand, $\beta_n(t)$ and $\phi(t)$ are related through the orthogonalization procedure,

$$\hat{\phi}(w) = M(w)\hat{\beta}_n(w),$$

and using the two-scale equation for β, we can rewrite the above equation as

$$\hat{\phi}(w) = M(w)H_b\left(\frac{w}{2}\right)\hat{\beta}_n\left(\frac{w}{2}\right) = M(w)H_b\left(\frac{w}{2}\right)\hat{\phi}\left(\frac{w}{2}\right)\Big/ M\left(\frac{w}{2}\right).$$

From this we immediately obtain an explicit expression for *H(w)*

$$H(w) = H_b(w)\frac{M(2w)}{M(w)} = e^{-iwK/2}\left(\cos\frac{w}{2}\right)^{n+1}\sqrt{\frac{(2\sin w/2)^{2(n+1)}\Sigma_{2(n+1)}(w)}{(2\sin w)^{2(n+1)}\Sigma_{2(n+1)}(2w)}}$$

$$= \frac{e^{-iwk/2}}{2^{n+1}}\sqrt{\frac{\Sigma_{2(n+1)}(w)}{\Sigma_{2(n+1)}(2w)}}sign(\cos^K \frac{w}{2}). \qquad (3.8)$$

The desired filter coefficients are given by $\sqrt{2}$ times the Fourier coefficients of *H(w)*:

$$h_k = \sqrt{2}\frac{1}{2\pi}\int_0^{2\pi} H(w)e^{ikw}dw.$$

Now we discuss the calculation of the corresponding mother wavelet $\psi(t)$. In principle, once the coefficients in the dilation equation $\{h_k\}$ are known, we can get the coefficients in the wavelet equation through $g_k = (-1)^k h_{1-k}$, and the mother wavelet can be obtained from the superposition of the dilated scaling function. However, since the nonorthogonal scaling function $\beta_n(t)$ is known directly, we can in this particular case also write the wavelet as a superposition of $\{\beta_n(t-k)\}$ rather than that of $\{\phi(t-k)\}$. From the wavelet equation, we have

$$\hat{\psi}(w) = G(w/2)\hat{\phi}(w/2) = -e^{-iw/2}\overline{H(w/2+\pi)}\hat{\phi}(w/2) \tag{3.9}$$

If we define

$$N(w/2) \equiv \frac{M(w)M(w/2)}{M(w/2+\pi)},$$

$$G_b(w/2) \equiv -e^{-iw/2}\overline{H_b(w/2+\pi)},$$

and

$$\hat{\beta}_n^{\#} \equiv G_b(w)\hat{\beta}_n(w),$$

the above expression (3.9) can be written as

$$\hat{\psi}(w) = N\left(\frac{w}{2}\right)G_b\left(\frac{w}{2}\right)\hat{\beta}_n\left(\frac{w}{2}\right) = N\left(\frac{w}{2}\right)\hat{\beta}_n^{\#}\left(\frac{w}{2}\right),$$

and the wavelet can then be obtained from

$$\psi(t) = \sum_k n_k \beta_n^{\#}(2t-k) = \sum_k n_k \sum_l g_l \beta_n(2t-k-l) = \sum_k \sum_l n_{k-l} g_l \beta_n(2t-k).$$

The coefficients $\{n_k\}$ are obtained by Fourier transforming $N(w) = \sum_k n_k / 2e^{-ikw}$ and the coefficients $\{g_k\}$ are given by $g_k = (-1)^k b_{1-k}/2$ where $\{b_k\}$ are the coefficients connecting $\beta_n(t)$ with $\beta_n(2t)$.

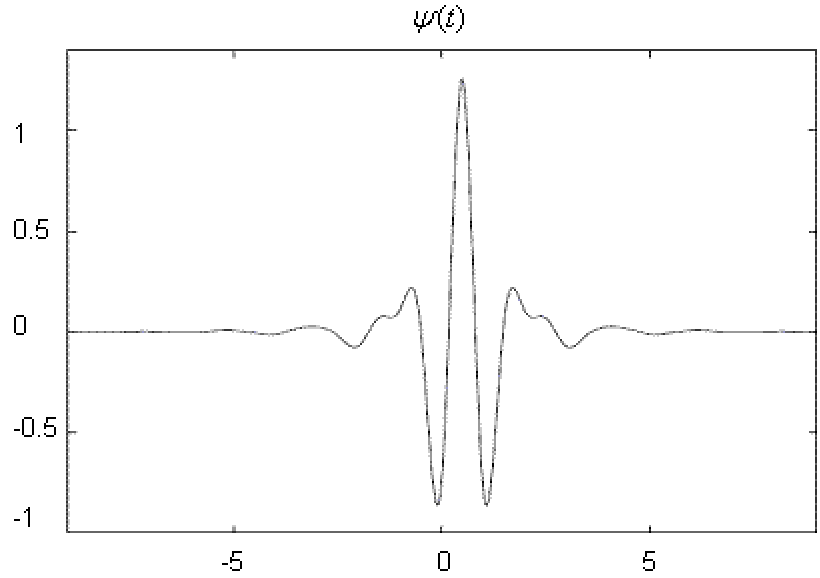

Figure 3.3. Spline wavelet

3.1.2. Shannon Wavelet

In the Haar system, the scaling function $\phi(t)$ is the box function and in Fourier space $\hat{\phi}(w)$ is, apart from a phase factor, $\sin\frac{w}{2}\bigg/\left(\frac{w}{2}\right)$ (Chau, 2004). Now if we reverse the roles of $\phi(t)$ and $\hat{\phi}(w)$ and let

$$\hat{\phi}(w)=\begin{cases}1 & -\pi\le w<\pi\\ 0 & otherwise\end{cases}$$

then

$$\phi(t)=\frac{1}{2\pi}\int_{-\infty}^{\infty}\hat{\phi}(w)e^{iwt}dw=\frac{1}{2\pi}\int_{-\pi}^{\pi}e^{iwt}dw=\frac{\sin\pi t}{\pi t} \tag{3.10}$$

In order to see that the above $\phi(t)$ is indeed a scaling function associated with a multiresolution analysis, we first introduce the idea of band-limited functions. A function $f(t)\in L^2(R)$ is *band limited* if its Fourier transform $\hat{f}(w)$ is zero when w is outside certain frequency band, that is, $|w| > \Omega$. It is well known that a band-limited function can be expressed as

$$f(t) = \sum_n f\left(\frac{\pi}{\Omega}n\right)\frac{\sin(\Omega t - \pi n)}{\Omega t - \pi n} \tag{3.11}$$

This is called the *Shannon sampling theorem*. It says that a band-limited function can be recovered from its discrete sample points. The above identity can be shown by first writing $\hat{f}(w)$ in terms of its Fourier series:

$$\hat{f}(w) = \sum_n c_n e^{-i\frac{\pi}{\Omega}nw} \quad for \ \ |w| \le \Omega$$

where

$$c_n = \frac{1}{2\Omega}\int_{-\Omega}^{\Omega}\hat{f}(w)e^{i\frac{\pi}{\Omega}nw}dw = \frac{\pi}{\Omega}\frac{1}{2\pi}\int_{-\infty}^{\infty}\hat{f}(w)e^{i\left(\frac{\pi}{\Omega}n\right)w}dw = \frac{\pi}{\Omega}f\left(\frac{\pi}{\Omega}n\right).$$

On the other hand,

$$f(t) = \frac{1}{2\pi}\int_{-\infty}^{\infty}\hat{f}(w)e^{iwt}dw = \frac{1}{2\pi}\int_{-\Omega}^{\Omega}\hat{f}(w)e^{iwt}dw$$

$$= \frac{1}{2\pi}\sum_n c_n\int_{-\Omega}^{\Omega}e^{i\left(t-n\frac{\pi}{\Omega}\right)w}dw = \sum_n f\left(\frac{\pi}{\Omega}n\right)\frac{\sin(\Omega t - \pi n)}{\Omega t - \pi n}$$

If we let V_0 be the space of functions $f(t) \in L^2(R)$ whose Fourier transform $\hat{f}(w)$ vanishes for $|w| > \pi$, then from the Shannon sampling theorem (3.11), *f(t)* can be written as (setting $\Omega = \pi$)

$$f(t) = \sum_n f(n) \frac{\sin \pi (t-n)}{\pi (t-n)}$$

This says that the functions $\{\phi(t-n) = \left\{ \frac{\sin \pi (t-n)}{\pi (t-n)} \right\}$ form a basis for V_0 . The basis is also orthonormal since we can easily check that $\sum_l \left| \hat{\phi}(w + 2\pi l) \right|^2 = 1$.

The multiresolution analysis consists of spaces $\{V_j\}$ that are scaled versions of V_0. For example, the space V_1 consists of all square integrable functions whose Fourier transforms vanish for $|w| > 2\pi$. Obviously $V_0 \subset V_1$. If $f(t) \in V_0$, we need to show that $g(t) = f(2t) \in V_1$, and vice versa. Since

$$g(t/2) = f(t) = \sum_n f(n) \frac{\sin \pi (t-n)}{\pi (t-n)} = \sum_n g(n/2) \frac{\sin \pi (t-n)}{\pi (t-n)},$$

we have

$$g(t) = \sum_n g(n/2) \frac{\sin \pi (2t-n)}{\pi (2t-n)}.$$

That is, $g(t) = f(2t)$ is a band-limited function with $\Omega = 2\pi$. Similarly, we can complete the proof that $\{V_j\}$ form a multiresolution analysis with the scaling function

$$\phi(t) = \sin \pi t / \pi t.$$

This is called the Shannon multiresolution analysis.

Next we look at the response function *H(w)*. The dilation equation in Fourier space is

$$\hat{\phi}(w) = H\left(\frac{w}{2}\right) \hat{\phi}\left(\frac{w}{2}\right).$$

Since $\hat{\phi}\left(\frac{w}{2}\right)=1$ for $-2\pi \le w < 2\pi$ and zero elsewhere, we can identify $H(w/2)=\hat{\phi}(w)$ on $w\in[-2\pi,\,2\pi]$, or $H(w)=\hat{\phi}(2w)$ on the interval $w\in[-\pi,\,\pi]$. However, the frequency response function *H(w)* ought to be 2π -periodic, so we "periodize" it by extending it periodically. This is accomplished by forming the infinite sum

$$H(w)=\sum_l \hat{\phi}(2(w+2\pi l)).$$

So we have,

$$\hat{\psi}(w)=-e^{-iw/2}\overline{H(w/2+\pi)}\hat{\phi}(w/2)=\begin{cases}-e^{-iw/2} & \pi \le |w| \le 2\pi \\ 0 & otherwise\end{cases},$$

and

$$\psi(t)=\frac{1}{2\pi}\int_{-\infty}^{\infty}\hat{\psi}(w)e^{iwt}dt=\frac{-1}{2\pi}\left(\int_{-2\pi}^{-\pi}e^{i(t-1/2)w}dw+\int_{\pi}^{2\pi}e^{i(t-1/2)w}dw\right)$$

$$=\frac{\sin\pi\left(t-\frac{1}{2}\right)-\sin 2\pi\left(t-\frac{1}{2}\right)}{\pi\left(t-\frac{1}{2}\right)} \tag{3.12}$$

This is referred to as the Shannon wavelet.

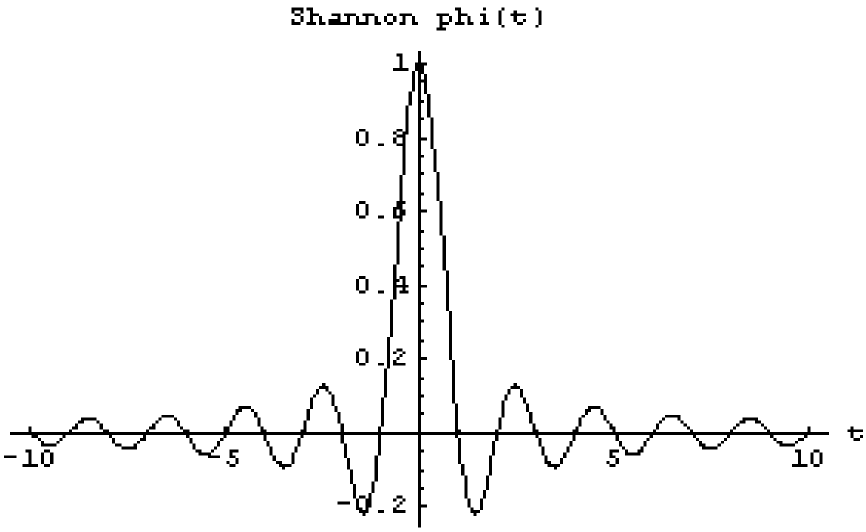

Figure 3.4. Shannon scaling function

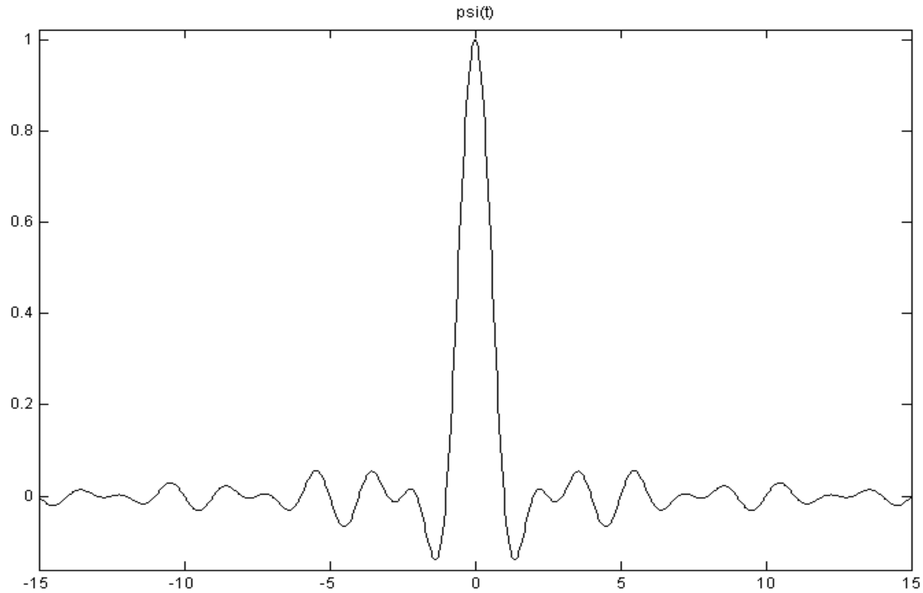

Figure 3.5. Shannon wavelet

We see that the scaling function and the wavelet decay very slowly in time. This is due to the discontinuities in $\hat{\phi}(w)$. The lack of smoothness of ϕ in frequency space gives rise to its poor localization in time. The Haar wavelet is just the opposite extreme where ϕ is discontinuous in time. The filter coefficients $\{h_k\}$ for Shannon wavelet decay as k^{-1}:

$$h_k = \sqrt{2}\frac{1}{2\pi}\int_{-\pi}^{\pi} H(w)e^{ikw}dw = \sqrt{2}\frac{1}{2\pi}\int_{-\pi/2}^{\pi/2} e^{ikw}dw$$

$$= \begin{cases} \dfrac{\sqrt{2}}{2} & k = 0 \\ \sqrt{2}\dfrac{(-1)^{(k-1)/2}}{\pi k} & k \ odd \\ 0 & otherwise \end{cases}$$

This slow decay of the filter coefficients makes Shannon wavelet less practical.

3.1.3. Meyer Wavelet

The slow decay of the Shannon wavelet in the time domain can be improved by smoothing the scaling function in frequency space. Instead of a sharp discontinuity, a smooth function is used to interpolate between $\hat{\phi}(w) = 1$ and $\hat{\phi}(w) = 0$ (Mallat, 1999). The Meyer scaling function is

$$\hat{\phi}(w) = \begin{cases} 1 & |w| \leq 2\pi/3 \\ \cos\left[\dfrac{\pi}{2}v\left(\dfrac{3}{2\pi}|w| - 1\right)\right] & 2\pi/3 \leq |w| \leq 4\pi/3 \\ 0 & otherwise \end{cases}$$

where v is a smooth function satisfying

$$v(x) = \begin{cases} 0 & if \ x \leq 0 \\ 1 & if \ x \geq 1 \end{cases},$$

and

$v(x)+v(1-x)=1$.

For example, we can choose *v(x)* for $x \in [0,1]$ to be a polynomial interpolating between 0 and 1. One choice is

$$v(x)=x^4(35-84x+70x^2-20x^3). \tag{3.13}$$

The fact that $\{\phi(t-k)\}$ form an orthonormal basis can be seen from $\sum_l \left|\hat{\phi}(w+2\pi l)\right|^2 =1$. We see that the supports of $\hat{\phi}(w)$ and $\phi(w-2\pi)$ only overlap in the region $w \in [2\pi/3, 4\pi/3]$, so we only need to show that

$$\cos^2\left[\frac{\pi}{2}v\left(\frac{3}{2\pi}w-1\right)\right]+\cos^2\left[\frac{\pi}{2}v\left(\frac{3}{2\pi}|w-2\pi|-1\right)\right]=1.$$

This is true since the second term on the left-hand side of the equation can be written as

$$\cos^2\left[\frac{\pi}{2}v\left(-\frac{3}{2\pi}w+2\right)\right]=\cos^2\left[\frac{\pi}{2}-\frac{\pi}{2}v\left(\frac{3}{2\pi}w-1\right)\right]=\sin^2\left[\frac{\pi}{2}v\left(\frac{3}{2\pi}w-1\right)\right]$$

So $\sum_l \left|\hat{\phi}(w+2\pi l)\right|^2 =1$. As in the last example, we take V_0 to be the closed space spanned by the orthonormal basis $\{\phi(t-k)\}$, and a multiresolution analysis can be constructed. The dilation equation gives

$$\hat{\phi}(w)=H\left(\frac{w}{2}\right)\hat{\phi}\left(\frac{w}{2}\right)=\hat{\phi}(w)\hat{\phi}(w/2).$$

Since $H(w)$ needs to be 2π -periodic, we again extend it periodically by forming the sum

$$H(w) = \sum_l \hat{\phi}(2(w + 2\pi l))$$

and $\hat{\psi}(w)$ is given by

$$\hat{\psi}(w) = G(w/2)\hat{\phi}(w/2) = -e^{-iw/2}\overline{H(w/2+\pi)}\hat{\phi}(w/2) = -e^{-iw/2}\sum_l \hat{\phi}(w + 2\pi + 4\pi l)\hat{\phi}(w/2)$$

Since the support of $\hat{\phi}(w/2)$ is $[-8\pi/3,\ 8\pi/3]$, only *l=0* and *l=-1* terms contribute to the above sum, and we have

$$\hat{\psi}(w) = -e^{-iw/2}(\hat{\phi}(w - 2\pi) + \hat{\phi}(w + 2\pi))\hat{\phi}(w/2)\ .$$

In addition, $\hat{\psi}(w)$ can be written as

$$\hat{\psi}(w) = \begin{cases} -e^{-iw/2}\sin\left[\frac{\pi}{2}v\left(\frac{3}{2\pi}|w| - 1\right)\right] & \frac{2\pi}{3} \le |w| \le \frac{4\pi}{3} \\ -e^{-iw/2}\cos\left[\frac{\pi}{2}v\left(\frac{3}{4\pi}|w| - 1\right)\right] & \frac{4\pi}{3} \le |w| \le \frac{8\pi}{3} \\ 0 & otherwise \end{cases}$$

The scaling function and wavelet in the time domain are obtained by doing the Fourier transforms:

$$\phi(t) = \frac{1}{2\pi}\int_{-\infty}^{\infty}\hat{\phi}(w)e^{iwt}dw = \frac{1}{\pi}\int_0^{4\pi/3}\hat{\phi}(w)\cos(wt)dw$$

and

$$\hat{\psi}(w) = -\frac{1}{2\pi}\int_{-\infty}^{\infty} e^{-iw/2}\hat{\phi}(w/2)\left[\hat{\phi}(w+2\pi)+\hat{\phi}(w-2\pi)\right]e^{iwt}\,dw$$

$$= -\frac{1}{\pi}\int_{0}^{\infty}\hat{\phi}(w/2)\hat{\phi}(w-2\pi)\cos w\left(t-\frac{1}{2}\right)dw$$

$$= -\frac{1}{\pi}\int_{2\pi/3}^{8\pi/3}\hat{\phi}(w/2)\hat{\phi}(w-2\pi)\cos w\left(t-\frac{1}{2}\right)dw$$

In general, we cannot get an analytic form for the scaling function or wavelet, and here we are content to approximate them using summations instead of integrals in the Fourier transform formula and plot them. We will call *n* the order of Meyer ϕ and ψ. The integrals are approximated by a summation with intervals of size $2\pi/(3k)$.

For example, here is the Meyer $\phi(t)$ when $v(x)=x$ for $x\in[0,1]$.

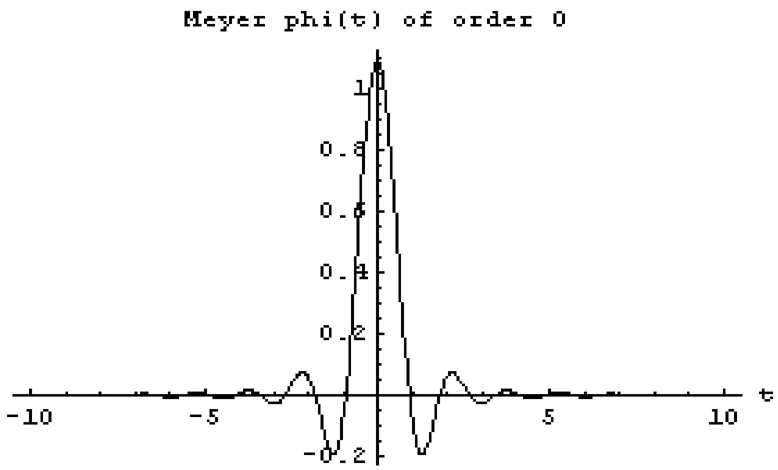

Figure 3.6. Meyer scaling function

Here is the corresponding wavelet $\psi(t)$. We see that as expected the scaling function and wavelet decay faster than in the case of the Shannon wavelet.

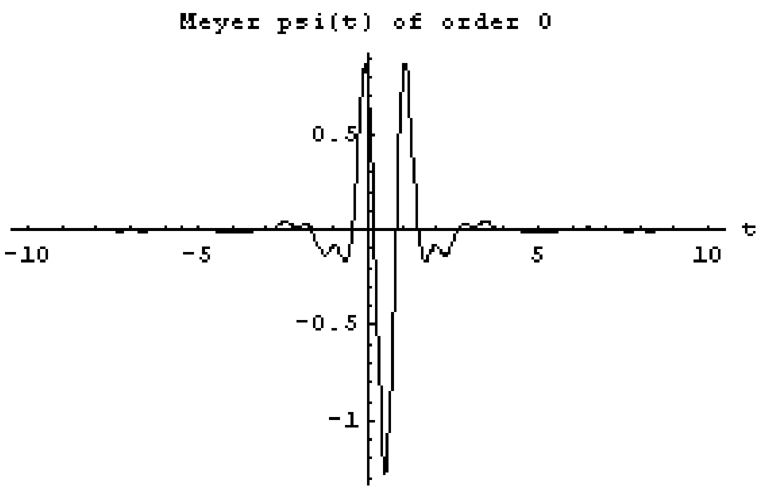

Figure 3.7. Meyer wavelet function

The filter coefficients $\{h_k\}$ are given by the Fourier transform of $H(w)$:

$$h_k = \sqrt{2}\,\frac{1}{2\pi}\int_{-\pi}^{\pi} H(w)e^{jkw}dw = \sqrt{2}\,\frac{1}{2\pi}\int_{-\pi}^{\pi}\hat{\phi}(2w)\cos(kw)dw$$

$$= \sqrt{2}\,\frac{1}{\pi}\left[\int_{0}^{\pi/3}\cos(kw)dw + \int_{\pi/3}^{2\pi/3}\cos\left[\frac{\pi}{2}v\left(\frac{3}{\pi}w-1\right)\right]\cos(kw)dw\right]$$

and they do not have an analytic form for a general $v(x)$. In the case of $v(x) = x$, that is, linear interpolation between $\hat{\phi}(w) = 0$ and $\hat{\phi}(w) = 1$, the filter coefficients can be calculated explicitly:

$$\begin{aligned} h_k &= \sqrt{2}\,\frac{1}{\pi}\left[\int_{0}^{\pi/3}\cos(kw)dw + \int_{\pi/3}^{2\pi/3}\cos\left[\frac{\pi}{2}v\left(\frac{3}{\pi}w-1\right)\right]\cos(kw)dw\right] \\ &= \frac{\sqrt{2}}{\pi}\left(\frac{\sin \pi k/3}{k} + \frac{4k\sin \pi k/3}{9-4k^2} + \frac{6\cos 2\pi k/3}{9-4k^2}\right) \end{aligned} \tag{3.14}$$

When k is large, the first two terms in (3.14) cancel and the coefficients decay as k^{-2}. The smoother the $\hat{\phi}(w)$, the faster the filter coefficients decay.

3.2. Biorthogonal Wavelets

In the case of the biorthogonal wavelet filters, the low pass and the high pass filters do not have the same length. The low pass filter is always symmetric, while the high pass filter could be either symmetric or anti-symmetric. The coefficients of the filters are either real numbers or integers (Mertins, 1999).

For perfect reconstruction, biorthogonal filter bank has all odd length or all even length filters. The two analysis filters can be symmetric with odd length or one symmetric and the other anti symmetric with even length. Also, the two sets of analysis and synthesis filters must be dual (Strang and Nguyen, 1997). The linear phase biorthogonal filters are the most popular filters for data compression applications.

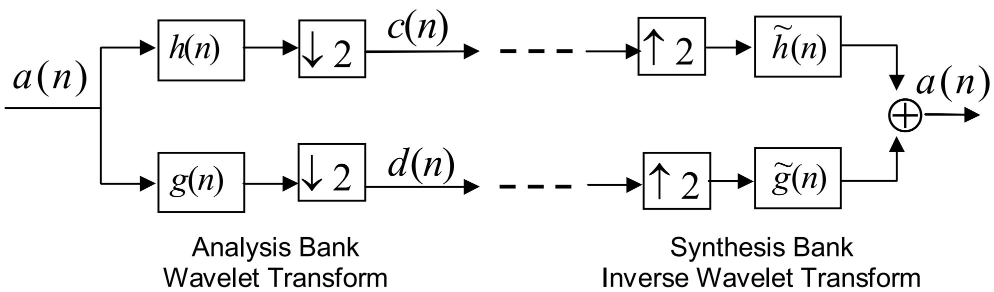

Figure 3.8. 2-Band Filter Banks

The scaling functions satisfy the double scaling equations:

$$\phi(t) = \sqrt{2}\sum_{n\in Z} h_n \phi(2t-n)$$

$$\tilde{\phi}(t) = \sqrt{2}\sum_{n\in Z} \tilde{h}_n \tilde{\phi}(2t-n)$$

Define the function m_0 as follows:

$$m_0(w) = \frac{1}{\sqrt{2}} \sum_{n \in Z} h_n e^{-ikw} = \frac{1}{\sqrt{2}} H(w) \tag{3.15}$$

The function m_0 is sometimes called the transfer function and it describes the behavior of the associated filter h in the Fourier domain (Lin, Shi, Hao and Xu, 2003). Notice that the function m_0 is 2π -periodic and that filter taps $\{h_n,\ n \in Z\}$ are in fact the Fourier coefficients in the Fourier series of

$$H(w) = \sqrt{2} m_0(w)$$

In the Fourier domain the relation $\phi(t)$ becomes

$$\phi(w) = m_0\left(\frac{w}{2}\right)\phi\left(\frac{w}{2}\right)$$

where $\phi(w)$ is the Fourier transform of $\phi(t)$. By iterating $\phi(w)$, one gets

$$\phi(w) = \prod_{n=1}^{\infty} m_0\left(\frac{w}{2^n}\right) \tag{3.16}$$

which is convergent under very mild conditions concerning the rates of decay of the scaling function ϕ .

The corresponding wavelet functions are

$$\psi(t) = \sqrt{2} \sum_{n \in z} g_n \phi(2t - n)$$

$$\widetilde{\psi}(t) = \sqrt{2} \sum_{n \in z} \widetilde{g}_n \widetilde{\phi}(2t - n)$$

$$g_n = (-1)^n \tilde{h}_{1-n} \quad , \quad \tilde{g}_n = (-1)^n h_{1-n} \tag{3.17}$$

Define the function m_1 as follows:

$$m_1(w) = \frac{1}{\sqrt{2}} \sum_{n \in Z} g_n e^{-ikw}$$

In the Fourier domain the relation $\psi(t)$ becomes,

$$\psi(w) = m_1\left(\frac{w}{2}\right)\phi\left(\frac{w}{2}\right) \tag{3.18}$$

3.2.1. Properties of Biorthogonal Wavelets

- Low-pass and high-pass conditions:

$$\sum_{n \in Z} h_n = \sum_{n \in Z} \tilde{h}_n = \sqrt{2} \quad , \quad \sum_{n \in Z} g_n = \sum_{n \in Z} \tilde{g}_n = 0 \tag{3.19}$$

- Linear phase property (or symmetry):

$$h_{-n} = h_n \, , \; \tilde{h}_{-n} = \tilde{h}_n \, , \; n \in Z$$

- Biorthogonal conditions:

$$\sum_{n \in Z} h_n \tilde{h}_{n-2j} = \delta_j \quad , \quad j \in Z \tag{3.20}$$

$$\sum_{n \in Z} g_n \tilde{g}_{n-2j} = \delta_j \quad , \quad j \in Z \tag{3.21}$$

$$\sum_{n\in Z} h_n \tilde{g}_{n-2j} = 0 \;, \quad j \in Z \tag{3.22}$$

$$\sum_{n\in Z} g_n \tilde{h}_{n-2j} = 0 \;, \quad j \in Z \tag{3.23}$$

$$g_n = (-1)^n \tilde{h}_{1-n} \;, \;\; \tilde{g}_n = (-1)^n h_{1-n}$$

- Decomposition (a => c + d):

$$c_k = \sum_{n\in Z} h_{n-2k} a_n \;, \qquad k \in Z$$

$$d_k = \sum_{n\in Z} g_{n-2k} a_n \;, \qquad k \in Z$$

- Reconstruction (c + d => a):

$$a_n = \sum_{k\in Z} \tilde{h}_{n-2k} c_k + \sum_{k\in Z} \tilde{g}_{n-2k} d_k \qquad n \in Z$$

- Perfect reconstruction (PR) condition is

$$\sum_{k\in Z} \tilde{h}_{n-2k} h_{m-2k} + \sum_{k\in Z} \tilde{g}_{n-2k} g_{m-2k} = \delta_{m,n} \;, \quad m, n \in Z \tag{3.24}$$

which is proved to be equivalent to

$$\sum_{n\in Z} h_n \tilde{h}_{n-2j} = \delta_j \;, \quad j \in Z$$

4. FILTER BANKS

For most signal and image processing applications, Discrete Wavelet Transform (DWT)-based analysis is best described in terms of filter banks. The use of a group of filters to divide up a signal into various spectral components is termed *subband coding* (Fliege, 1996). The most basic implementation of the DWT uses only two filters as in the filter bank shown in Figure 4.1.

The waveform under analysis is divided into two components. $y_{lp}(n)$ and $y_{hp}(n)$. by the digital filters $H_0(w)$ and $H_1(w)$. The spectral characteristics of the two filters must be carefully chosen with $H_0(w)$ having a lowpass spectral characteristic and $H_1(w)$ a highpass spectral characteristic. The highpass filter is analogous to the application of the wavelet to the original signal, while the lowpass filter is analogous to the application of the scaling or smoothing function. If the filters are invertible filters then it is possible, at least in theory, to construct complementary filters (filters that have a spectrum the inverse of $H_0(w)$ and $H_1(w)$) that will recover the original waveform from either of the subband signals, $y_{lp}(n)$ or $y_{hp}(n)$. The original signal can often be recovered even if the filters are not invertible, but both subband signals will need to be used. Signal recovery is illustrated in Figure 4.2 where a second pair of filters. $G_0(w)$ and $G_1(w)$, operate on the high and lowpass subband signals and their sum is used to reconstruct a close approximation of the original signal, $x^{'}(t)$. The Filter Bank that decomposes the original signal is usually termed the *analysis filters* while the filter bank that reconstructs the signal is termed the *syntheses filters.* FIR filters are used throughout because they are inherently stable and easier to implement.

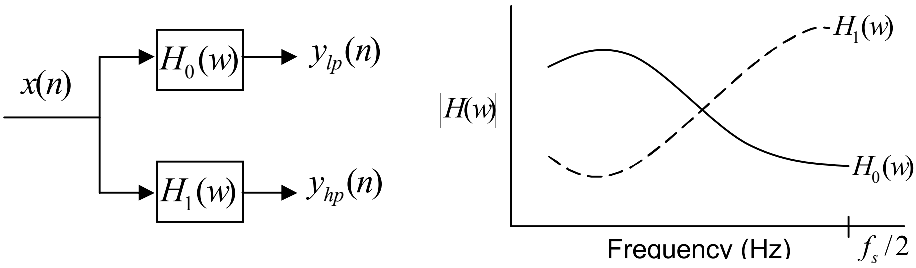

Figure 4.1. Simple filter bank consisting of only two filters applied to the same waveform. The filters have lowpass and highpass spectral characteristics. Filter outputs consist of a lowpass subband, $y_{lp}\{n)$, and a highpass subband, $y_{hp}(n)$.

Filtering the original signal, *x(n),* only to recover it with inverse filters would be a pointless operation. In some analysis applications only the subband signals are of interest and reconstruction is not needed, but in many wavelet applications, some operation is performed on the subband signals, $y_{lp}(n)$ and $y_{hp}(n)$, before reconstruction of the output signal (see Figure 4.2). In such cases, the output will no longer be exactly the same as the input. If the output is essentially the same, as occurs in some data compression applications, the process is termed *lossless,* otherwise it is a *lossy* operation.

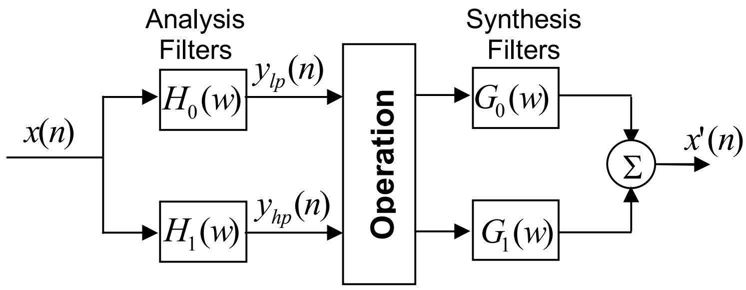

Figure 4.2. A typical wavelet application using filter banks containing only two filters. The input waveform is first decomposed into subbands using the *analysis filter* bank. Some process is applied to the filtered signals before reconstruction. Reconstruction is performed by the *synthesis filter* bank.

There is one major concern with the general approach schematized in Figure 4.2 it requires the generation of, and operation on, twice as many points as are in the original waveform *x(n)*. This problem will only get worse if more filters are added to the filter bank. Clearly there must be redundant information contained in signals $y_{lp}(n)$ and $y_{hp}(n)$, since they are both required to represent x(n). but with twice the number of points. If the analysis filters are correctly chosen, then it is possible to reduce the length of $y_{lp}(n)$ and $y_{hp}(n)$ by one half and still be able to recover the original waveform. To reduce the signal samples by one half and still represent the same overall time period, we need to eliminate every other point, say every odd point. This operation is known as *downsampling* and is illustrated schematically by the symbol ↓2. The downsampled version of *y(n)* would then include only the samples with even indices [y(2), y(4), y(6) …] of the filtered signal (Strang and Nguyen, 1997).

If downsampling is used, then there must be some method for recovering the missing data samples (those with odd indices) in order to reconstruct the original signal. An operation termed *upsampling* (indicated by the symbol ↑2) accomplishes this operation by replacing the missing points with zeros. The recovered signal *(x'{n)* in Figure 4.2) will not contain zeros for these data samples as the synthesis filters, $G_0(w)$ or $G_1(w)$, fill in the blanks. Figure 4.3 shows a wavelet application that uses three filter banks and includes the downsampling and upsampling operations. Downsampled amplitudes are sometimes scaled by $\sqrt{2}$, a normalization that can simplify the filter calculations when matrix methods are used.

Designing the filters in a wavelet filter bank can be quite challenging because the filters must meet a number of criteria. A prime concern is the ability to recover the original signal after passing through the analysis and synthesis filter banks. Accurate recovery is complicated by the downsampling process (Vetterli and Herley, 1992). Note that downsampling, removing every other point, is equivalent to sampling the original signal at half the sampling frequency. For some signals, this would lead to aliasing, since the highest frequency component in the signal may no longer be twice the now reduced sampling frequency. Appropriately chosen filter banks can essentially cancel potential aliasing. If the filter bank contains only two filter types (highpass and lowpass filters) as in Figure 4.2, the criterion for aliasing cancellation is

$$G_0(z)H_0(-z)G_1(z)H_1(-z) = 0 \tag{4.1}$$

where $H_0(z)$ is the transfer function of the analysis lowpass filter. $H_1(z)$ is the transfer function of the analysis highpass filter. $G_0(z)$ is the transfer function of the synthesis lowpass filter, and $G_1(z)$ is the transfer function of the synthesis highpass filter.

The requirement to be able to recover the original waveform from the subband waveforms places another important requirement on the filters which is satisfied when:

$$G_0(z)H_0(z)G_1(z)H_1(z) = 2z^{-N} \tag{4.2}$$

where the transfer functions are the same as those in Eq. (4.1). N is the number of filter coefficients (i.e.. the filter order); hence z^{-N} is just the delay of the filter (Tran, Quetroz and Nguyen, 2000).

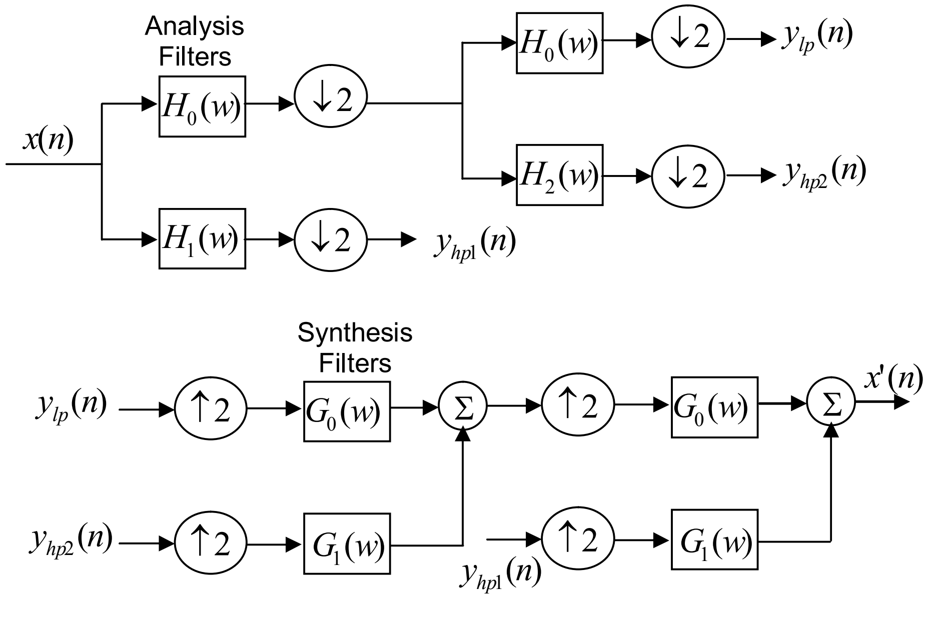

Figure 4.3. A typical wavelet application using three filters. The downsampling (↓2) and upsampling (↑2) processes are shown.

In order for the highpass filter output to be orthogonal to that of the low-pass output, the highpass filter frequency characteristics must have a specific relationship to those of the lowpass filter:

$$H_1(z) = -z^{-N} H_0(-z^{-1}) \tag{4.3}$$

The criterion represented by Eq. (4.3) can be implemented by applying the alternating flip algorithm to the coefficients of $h_0(n)$:

$$h_1(n) = [h_0(N), -h_0(N-1), h_0(N-2), -h_0(N-3), \ldots] \tag{4.4}$$

where N is the number of coefficients in $h_0(n)$.

The conditions of Eq. (4.2) can be met by making $G_0(z) = H_1(-z)$ and $G_1(z) = -H_0(-z)$ Hence the synthesis filter transfer functions are related to the analysis transfer functions by the Eqs. (4.5) and (4.6):

$$G_0(z) = H_1(z) = -z^{-N} H_0(-z^{-1}) \tag{4.5}$$

$$G_1(z) = -H_0(-z) = z^{-N} H_1(z^{-1}) \tag{4.6}$$

where the second equality conies from the relationship expressed in Eq. (4.3). The operations of Eqs. (4.5) and (4.6) can be implemented several different ways, but the easiest way in MATLAB is to use the second equalities in Eqs. (4.5) and (4.6), which can be implemented using the *order flip* algorithm:

$$g_0(n) = [h_0(N), h_0(N-1), h_0(N-2), \ldots] \tag{4.7}$$

$$g_1(n) = [h_1(N), h_1(N-1), h_1(N-2), \ldots] \tag{4.8}$$

where, N is the number of filter coefficients.

Note that if the filters shown in Figure 4.3 are causal, each would produce a delay that is dependent on the number of filter coefficients. Such delays are expected and natural, and may have to be taken into account in the reconstruction process. However, when the data are stored in the computer it is possible to implement FIR filters without a delay.

5. ELECTROENCEPHALOGRAM (EEG)

The human brain is an extremely complicated network that contains about 10^{10} interconnected neurons. Each neuron consists of a central portion containing the nucleus, known as the cell body, and one or more structures referred to as axons and dendrites. The dendrites are rather short extensions of the cell body and are involved in the reception of stimuli. The axon, by contrast, is usually a single elongated extension (Hinrichs, 2004). Rapid signaling within the nervous system occurs by two primary mechanisms:

- **Within nerves and neurons by way of action potentials**. These action potentials consist on a rapid swing of the polarity of the neuron transmembrane voltage from negative to positive and back. These voltage changes result from changes in the permeability of the membrane to specific ions, the internal and external concentrations of which are in imbalance.
- **Between neurons by way of neurotransmitter diffusion across synapses**. The release of chemical neurotransmitter is triggered by the arrival of a nerve impulse (action potential). Receptors on the opposite side of the synaptic gap bind neurotransmitter molecules and respond by opening nearby ion channels in the post-synaptic cell membrane, causing ions to rush in or out and changing the local transmembrane potential of the cell and thus propagating the nervous impulse (Stencel, 1992).

Both synaptic and action potentials result in potential differences across the neuron membrane. These potentials and the resting potentials of the glia cells are the main contributors of the EEG signal (Hinrichs, 2004).

The human spontaneous EEG has the appearance of a noisy signal devoid of any dominant frequency. Nevertheless, the frequency decomposition of this signal manifests a rhythmicity occasionally interrupted by transient discharges. These rhythms and discharges are classified according to their location, frequency, amplitude, morphology, periodicity, and behavioral and functional correlates (Stencel, 1992).

EEG signals are recorded as potential differences between surface electrodes on the scalp. The recorded signal therefore depends on the positions of the individual electrodes and how they are paired. Most laboratories performing routine clinical evaluations use the International 10-20 System of electrode placement. This system is based on placing the electrodes at 10 % to 20 % of the distances between anatomical landmarks on the skull and head, with the idea of providing some standardization across head size. Each electrode site has a letter identifying its sub-cranial lobe (i.e. FP-Frontopolar or prefrontal lobe, F-Frontal lobe, T- Temporal lobe, C-Central lobe , P-Parietal lobe, O-Occipital lobe) and a number, or another letter identifying its hemispherical location. The subscript Z (denoting line zero) ensuing any lobe abbreviation, refers to an electrode placed along the cerebrums midline. The use of an even number (2, 4, 6 or 8) represents the right hemisphere, with odd numbers (1, 3, 5 or 7) referring to the left hemisphere. The numbers rise with increasing distance from the midline of the head. Figure 5.1 depicts the positions of the electrodes in the international 10-20 system (Hinrichs, 2004).

Apart from the electrodes any EEG recording system requires at least these elements:

- **Amplifiers**. Since the amplitude of the signals recorded in the scalp is typically in the range of 10-100 μV high input impedance differential amplifiers are required.
- **Filters**. Usually the EEG signal is filtered before recording it. High-pass, low-pass and notch filters are used in this context.
- **Recording unit**. Used to keep a permanent record of the EEG signal.

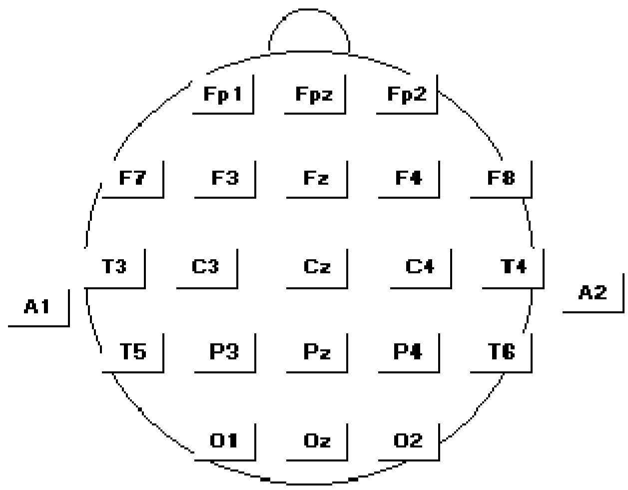

Figure 5.1. A single plane projection of the head on which the standard electrode sites of the international 10-20 system.

5.1. Excitatory Postsynaptic Potential (EPSP)

The electric potential of neurons is responsible for signal transmission. The inside of a neuron generally has an excess of negative charges. When a neuron is unstimulated, the difference in electric charge across the plasma membrane is the resting potential. A neuron is sensitive to physical or chemical changes that cause changes in the resting potential (Purves, Orians, Heler and Sadava,1998). A sudden and rapid reversal in charge across the membrane is called an action potential. When a neuron is stimulated, the action potential moves along the axon to the axon terminals to the target cell. The post-synaptic membrane of the target cell integrates the information it receives. In order for the target cell to be stimulated, the stimulus must be greater than the target cell's action potential. Neurotransmitters that affect the membrane bring about an excitatory postsynaptic potential (EPSP). When several EPSP's arrive at the cell body simultaneously, the potential is summed over the number of synaptic knobs, and an action potential may be reached (Stencel, 1992).

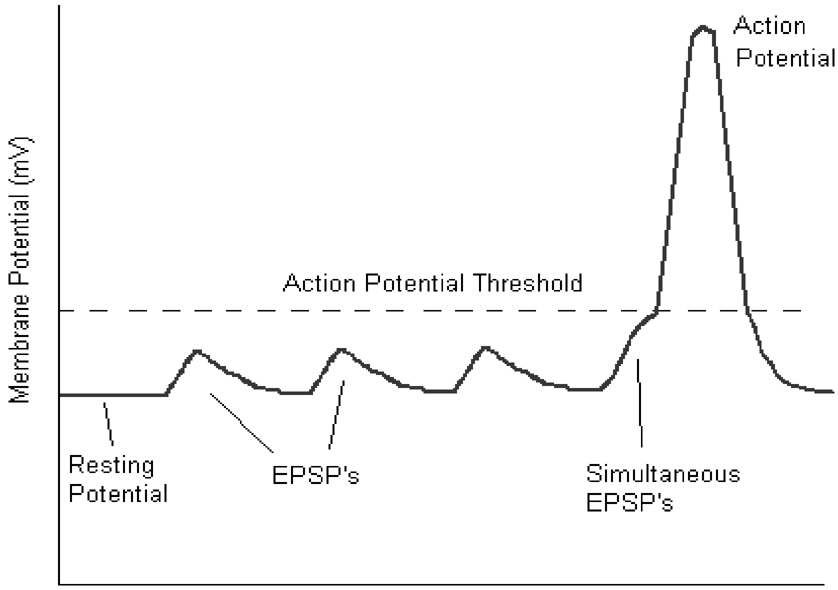

Figure 5.2. Excitatory Postsynaptic Potential (EPSP)

5.2. Wavelets in Electroencephalography Applications

Electroencephalographic waveforms such as EEG and event related potentials (ERP) recordings from multiple electrodes vary their frequency content over their time courses and across recording sites on the scalp. Accordingly, EEG and ERP data sets are nonstationary in both time and space. Furthermore, three specific components and events that interest neuroscientists and clinicians in these data sets tend to be transient (localized in time), prominent over certain scalp regions (localized in space), and restricted to certain ranges of temporal and spatial frequencies (localized in scale). Because of these characteristics, wavelets are suited for the analysis of the EEG and ERP signals (Semmlow, 2004). Wavelet based techniques can nowadays be found in many processing areas of neuroelectric waveforms, such as:

- **Noise filtering**. After performing the wavelets transform to a EEG or ERP waveform, precise noise filtering is possible simply by zeroing out or attenuating any wavelet coefficients associated primarily with noise and then reconstructing the neuroelectric signal using the inverse wavelet transform.

- **Preprocessing neuroelectric data for input to neural networks**. Several studies suggest that wavelet decompositions of neuroelectric waveforms may have important processing applications in intelligent detection systems for use in clinical and human performance settings.
- **Neuroelectric waveform compression**. Wavelet compression techniques have been shown to improve neuroelectric data compression ratios with little loss of signal information when compared with classical compression techniques. Furthermore, there are very efficient algorithms available for the calculation of the wavelet transform that make it very attractive from the computation requirements point of view.
- **Spike and transient detection**. As we already know, the wavelet representation has the property that its time or space resolution improves as the scale of a neuroelectric event decreases. This variable resolution property makes wavelets ideally suited to detect the time of occurrence and the location of small-scale transient events such as focal epileptogenic spikes
- **Component and event detection**. Wavelets methods, such as wavelets packets, offer precise control over the frequency selectivity of the decomposition, resulting in precise component identification, even when the components substantially overlap in time and frequency. Furthermore, wavelets shapes can be designed to match the shapes of components embedded in ERPs. Such wavelets are excellent templates to detect and separate those components and events from the background EEG.
- **Time-scale analysis of EEG waveforms**. Time-scale and space-scale representations permit the user to search for functionally significant events at specific scales, or to observe time and spatial relationships across scales.

6. DERIVING ORTHOGONAL SCALING FUNCTION FROM EPSP FUNCTION

We will now derive our multiresolution wavelet based EPSP function. The EPSP function is

$$epsp(t) = \frac{c.d}{d-c}\left(e^{-ct} - e^{-dt}\right) \tag{6.1}$$

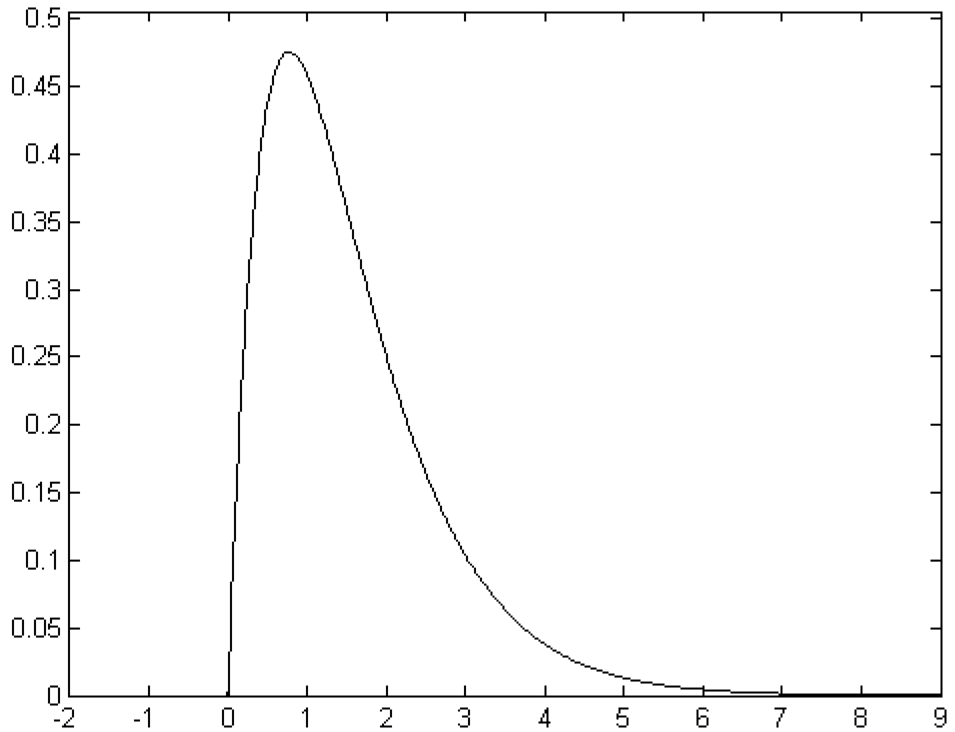

Figure 6.1. EPSP function

We get EPSP function as two scale or dilation equation. The Fourier transform of *epsp(t)* is

$$EPSP(w) = \int_{-\infty}^{\infty} epsp(t)e^{-iwt}dt = \int_{0}^{\pi} \frac{c.d}{d-c}\left(e^{-ct} - e^{-dt}\right)e^{-iwt}dt = \frac{c.d}{(c+iw).(d+iw)}. \tag{6.2}$$

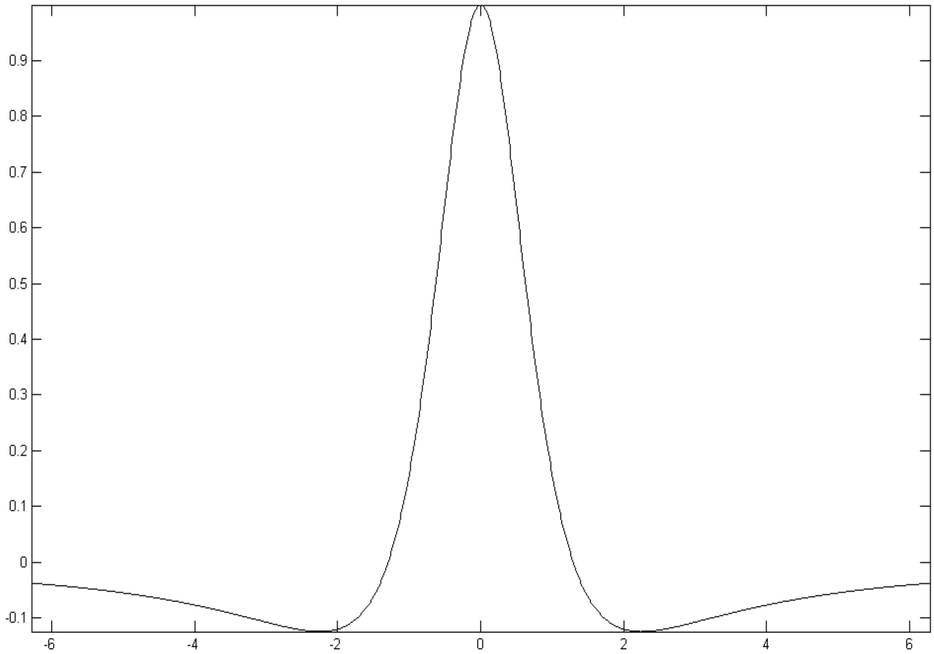

Figure 6.2. Fourier Transform of EPSP function

To orthogonalize $EPSP(w)$ it is useful to first calculate the quantity *b(w)* which is defined by

$$b(w) \equiv \sum_{l} \left| EPSP(w + 2\pi l) \right|^2 \qquad (6.3)$$

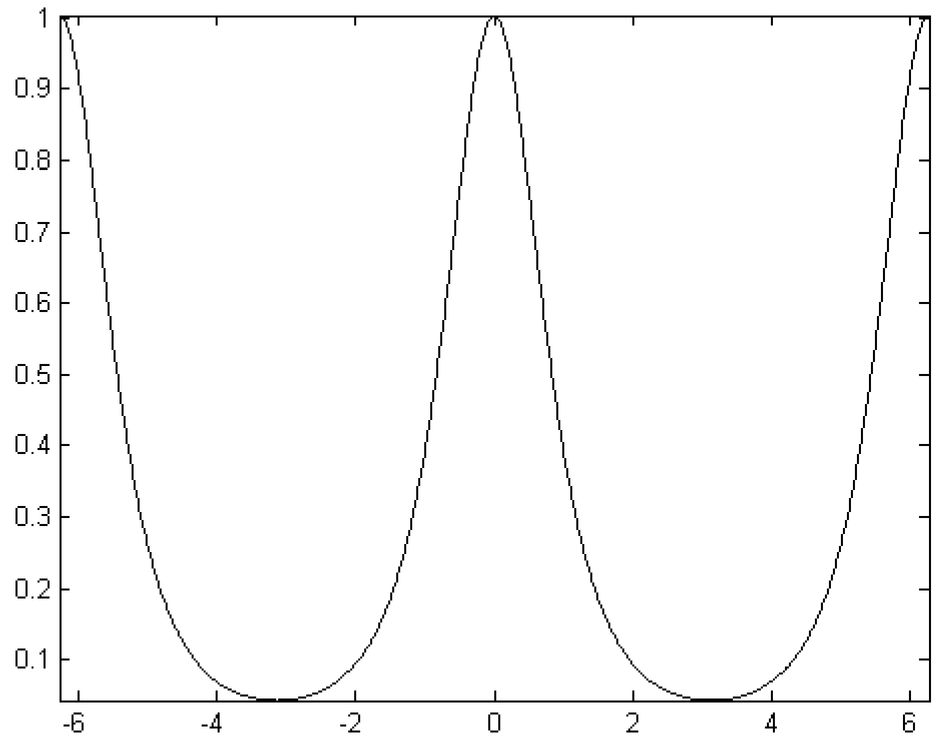

Figure 6.3. b(w)

The desired scaling function, that is, the orthogonalized EPSP function is, in Fourier space,

$$\hat{\phi}(w) = \frac{EPSP(w)}{\sqrt{b(w)}} = \frac{EPSP(w)}{\sqrt{\sum_{l=-\infty}^{\infty} \left| EPSP(w + 2\pi l) \right|^2}} \tag{6.4}$$

Where $1/\sqrt{b(w)}$ is an even, 2π -periodic function of *w*. To find the orthogonalized scaling function $\phi(t)$, the straightforward procedure is to apply the inverse Fourier transform to $\hat{\phi}(w)$. A simpler way of finding $\phi(t)$ is to find $\{p_k\}$, where

$$\phi(t) = \sum_k p_k epsp(t-k).$$

Where,

$$p_k = \frac{1}{2\pi}\int_{-\pi}^{\pi} \frac{1}{\sqrt{b(w)}} e^{jwk}\, dw$$

$$= \frac{1}{2\pi}\int_{0}^{\pi} \frac{1}{\sqrt{b(w)}} e^{jwk}\, dw + \frac{1}{2\pi}\int_{-\pi}^{0} \frac{1}{\sqrt{b(w)}} e^{jwk}\, dw$$

$$= \frac{1}{\pi}\int_{0}^{\pi} \frac{1}{\sqrt{b(w)}} \cos(wk) dw$$

The orthogonalized scaling function $\phi(t)$ will not have finite support. This means that in principle we need to calculate infinitely many $\{p_k\}$ in order to get $\phi(t)$.

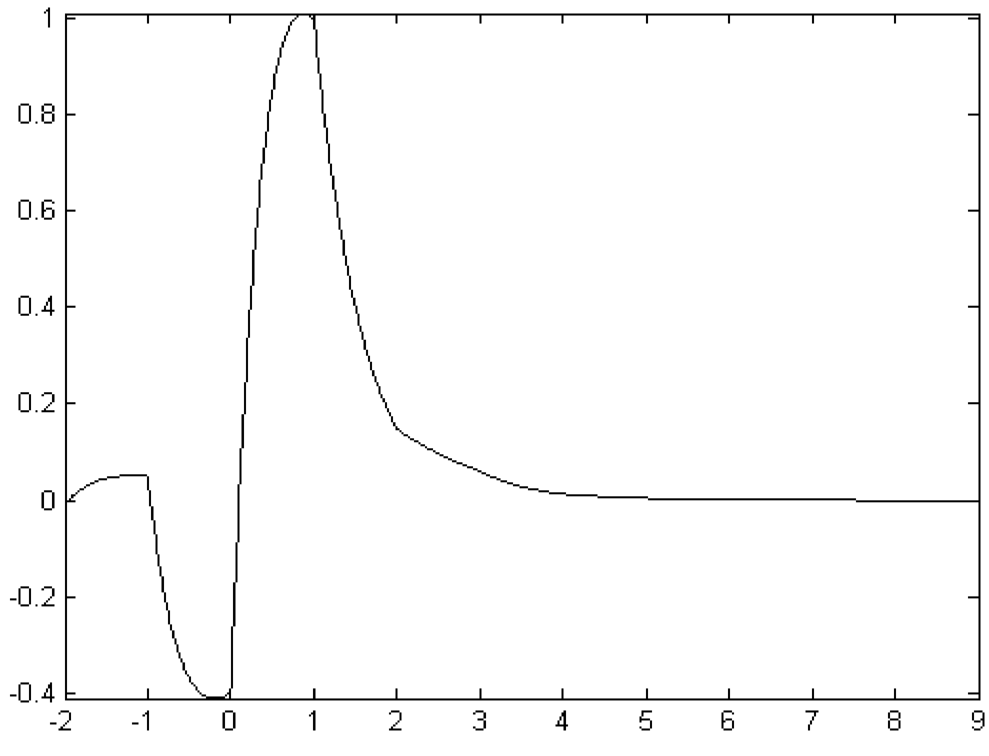

Figure 6.4. Orthogonalized scaling function

6.1. EPSP Filters and Wavelets

The mother wavelet $\psi(t)$ is obtained from the wavelet equation

$$\psi(t) = \sum_k \sqrt{2} g_k \phi(2t-k)$$

Where $\phi(t)$ is the scaling function of the multiresolution analysis and the coefficients $\{g_k\}$ are related to $\{h_k\}$ through

$$g_k = (-1)^k h_{1-k} .$$

$\{h_k\}$are the coefficients appearing in the dilation equation:

$$\phi(t) = \sum_k \sqrt{2} h_k \phi(2t-k) \ .$$

Therefore, once we know the scaling function, the mother wavelet $\psi(t)$ can be obtained if the coefficients $\{h_k\}$, called filter coefficients, are known.

We first describe the calculation of the spline filter coefficients. Recall that the dilation equation in Fourier space assumes the form

$$\hat{\phi}(w) = H\left(\frac{w}{2}\right)\hat{\phi}\left(\frac{w}{2}\right),$$

To find the expression for *H (w)* we employ the two-scale equation satisfied by $epsp(t)$. In Fourier space it is

$$EPSP(w) = He\left(\frac{w}{2}\right)EPSP\left(\frac{w}{2}\right) \tag{6.5}$$

This gives $EPSP(w) = \prod_{k=1}^{\infty} He\left(\frac{w}{2^k}\right) EPSP(0)$. (6.6)

Take $EPSP(0) = 1$.

The scaling function has a low-pass characteristic. It can be shown that integrating a scaling function yields

$$\int_{-\infty}^{\infty} epsp(t)dt = 1 . \tag{6.7}$$

$$epsp(t) = \int_{-\infty}^{\infty} \sum_{k=0}^{N-1} \sqrt{2} he_k epsp(2t-1)dt = 1$$

$$\underbrace{\sum_{k=0}^{N-1} \sqrt{2} he_k \int_{-\infty}^{\infty} epsp(2t-1)dt}_{1} = \frac{1}{2}\left(\sum_{k=0}^{N-1} \sqrt{2} he_k \underbrace{\int_{-\infty}^{\infty} epsp(u)du}_{1} \right),$$

$$\sum_{k=0}^{N-1} he_k = \sqrt{2}$$

Orthogonality : $\int_{-\infty}^{\infty} \phi(t)\phi(t-k)dt = \delta(k)$

$$= \int_{-\infty}^{\infty} \left(\sum_{l=0}^{N-1} \sqrt{2} he_l \phi(2t-l) \right)\left(\sum_{m=0}^{N-1} \sqrt{2} he_m \phi(2t-2k-m) \right) dt$$

$$= 2\sum_{m=0}^{N-1} \left(\sum_{l=0}^{N-1} he_l he_m \int_{-\infty}^{\infty} \phi(2t-l)\phi(2t-2k-m)dt \right)$$

$$= \left(\sum_{m=0}^{N-1} \left(\sum_{l=0}^{N-1} he_l he_m \int_{-\infty}^{\infty} \phi(u)\phi(u+l-m-2k)du \right) \right) = \delta(l-m-2k)\delta(k) \tag{6.8}$$

Hence,

$$\sum_{k=0}^{N-1} he_m he_{m+2k} = \delta(k) . \tag{6.9}$$

To find the filter coefficients he_k for epsp(t) we define y_k and b_k functions as

$$y_k = 2\sqrt{2}\sum_{k=0}^{N-1}\int_0^7 epsp(t)epsp(2t-k)dt \tag{6.10}$$

$$b_k = 4\sum_{k=0}^{N-1}\int_0^7 epsp(2t)epsp(2t-k)dt . \tag{6.11}$$

Hence

$$he_k = \frac{y_k}{b_k} . \tag{6.12}$$

On the other hand, $epsp(t)$ and $\phi(t)$ are related through the orthogonalization procedure,

$$\hat{\phi}(w) = \frac{EPSP(w)}{\sqrt{b(w)}} \tag{6.13}$$

and using the two-scale equation for *epsp*, we can rewrite the above equation as

$$\hat{\phi}(w) = \frac{1}{\sqrt{b(w)}} He\left(\frac{w}{2}\right) EPSP\left(\frac{w}{2}\right) = \frac{1}{\sqrt{b(w)}} He\left(\frac{w}{2}\right)\hat{\phi}\left(\frac{w}{2}\right)\sqrt{b\left(\frac{w}{2}\right)}$$

From this we obtain an explicit expression for *H(w)*

$$H(w) = He(w)\underbrace{\sqrt{\frac{b(w)}{b(2w)}}}_{P_0(w)} = He(w)P_o(w)\,.$$

$$h(n) = \sum_k p_{o\,k} he(n-k) \tag{6.14}$$

Where,

$$p_{ok} = \frac{1}{2\pi}\int_{-\pi}^{\pi}\sqrt{\frac{b(w)}{b(2w)}}e^{jwk}\,dw$$

$$= \frac{1}{2\pi}\int_{0}^{\pi}\sqrt{\frac{b(w)}{b(2w)}}e^{jwk}\,dw + \frac{1}{2\pi}\int_{-\pi}^{0}\sqrt{\frac{b(w)}{b(2w)}}e^{jwk}\,dw$$

$$= \frac{1}{\pi}\int_{0}^{\pi}\sqrt{\frac{b(w)}{b(2w)}}\cos(wk)dw.$$

Now we discuss the calculation of the corresponding mother wavelet $\psi(t)$. In principle, once the coefficients in the dilation equation $\{h_k\}$ are known, we can get the coefficients in the wavelet equation through $g_k = (-1)^k h_{1-k}$, and the mother wavelet can be obtained from the superposition of the dilated scaling function. From the wavelet equation, we have

$$\hat{\psi}(w) = G(w/2)\hat{\phi}(w/2) = -e^{-iw/2}\overline{H(w/2+\pi)}\hat{\phi}(w/2)$$

If we define

$$N(w/2) \equiv \sqrt{\frac{b(w/2+\pi)}{b(w)b(w/2)}}, \tag{6.15}$$

$$Ge(w/2) \equiv -e^{-iw/2}\,\overline{He(w/2+\pi)},$$

and

$$EPSPW(w) \equiv Ge(w)EPSP(w), \tag{6.16}$$

the above expression can be written as

$$\hat{\psi}(w) = N\left(\frac{w}{2}\right)Ge\left(\frac{w}{2}\right)EPSP\left(\frac{w}{2}\right) = N\left(\frac{w}{2}\right)EPSPW\left(\frac{w}{2}\right), \tag{6.17}$$

and the wavelet can then be obtained from

$$\psi(t) = \sum_k n_k epspw(2t-k) = \sum_k n_k \sum_l ge_l.epsp(2t-k-l) = \sum_k \sum_l n_{k-l} ge_l.epsp(2t-k).$$

The coefficients $\{n_k\}$ are obtained by Fourier transforming $N(w) = \sum_k n_k / 2e^{-ikw}$ and the coefficients $\{g_k\}$are given by $g_k = (-1)^k b_{1-k}/2$ where $\{b_k\}$ are the coefficients connecting $epsp(t)$ with $epsp(2t)$.

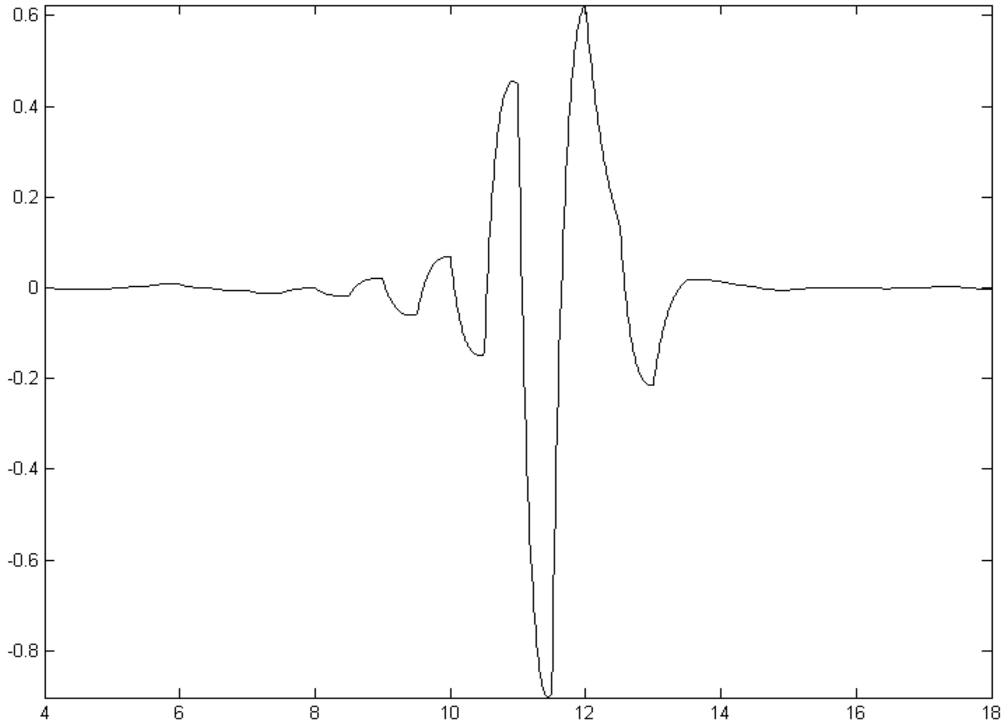

Figure 6.5. EPSP wavelet function

6.2. Comparison with Earlier Wavelets

We will now validate our multiresolution wavelet based EPSP function and illustrate it on synthetic (simulated) EEG signal with ERD and ERS events. It has only alpha and beta components.

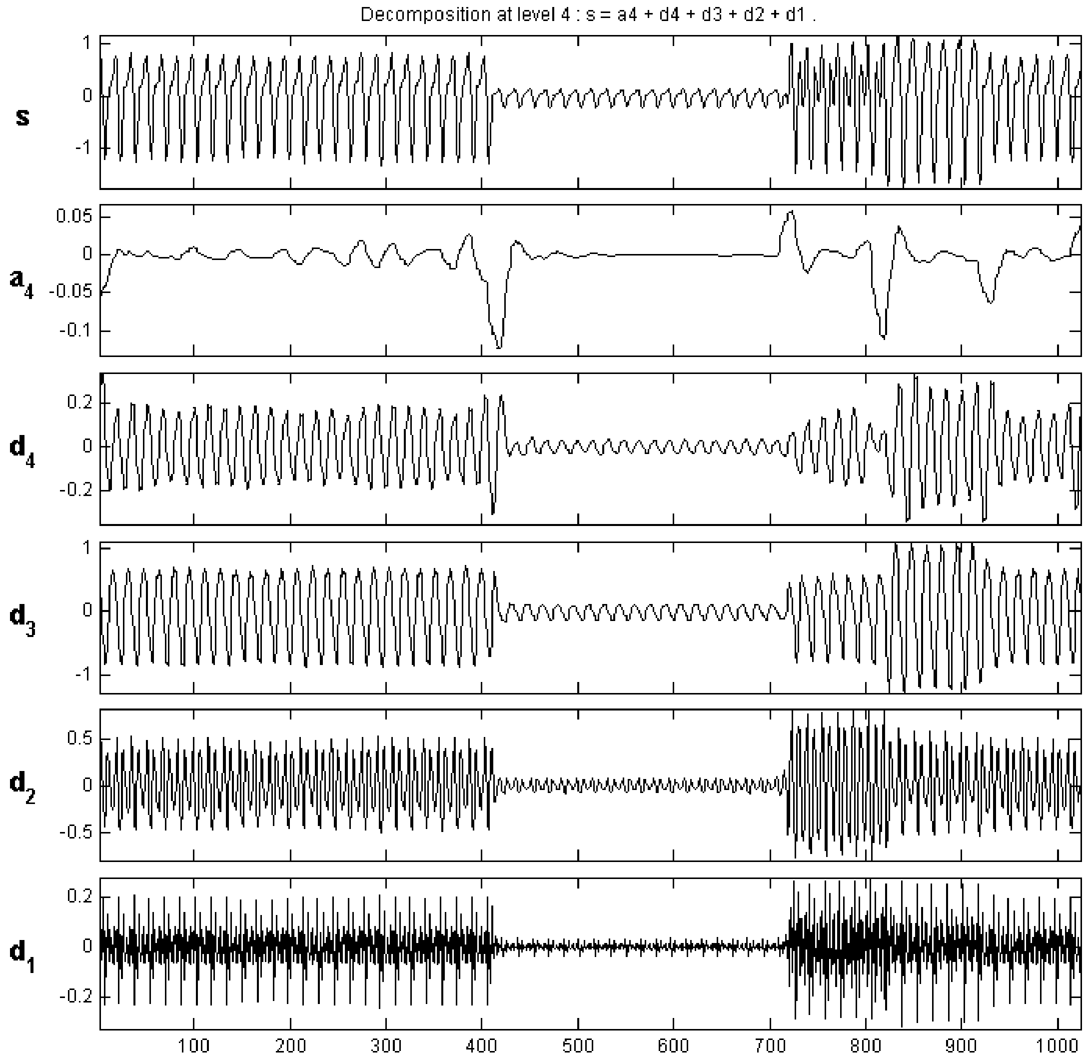

Figure 6.6. DWT decomposition of a EEG signal using EPSP wavelet

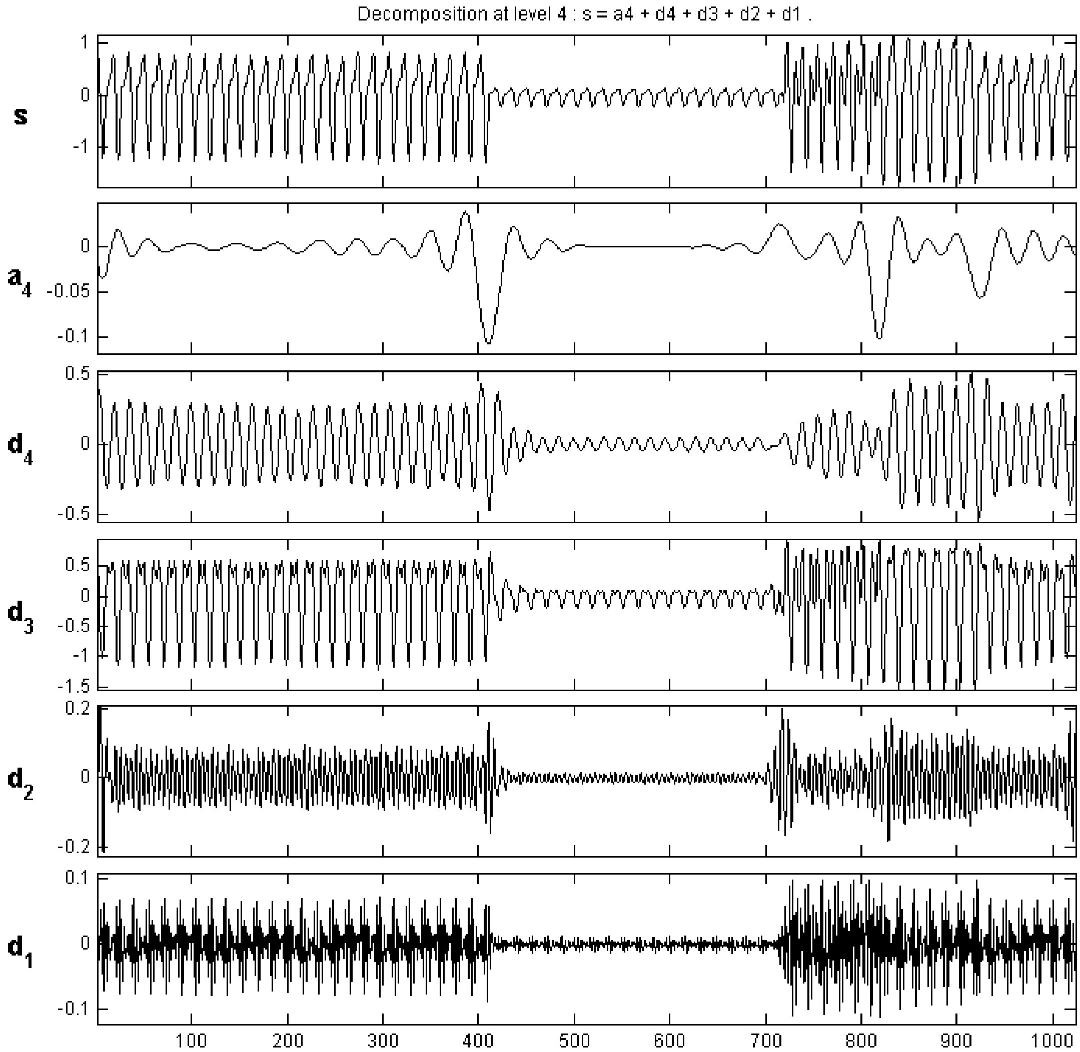

Figure 6.7. DWT decomposition of a EEG signal using Meyer wavelet

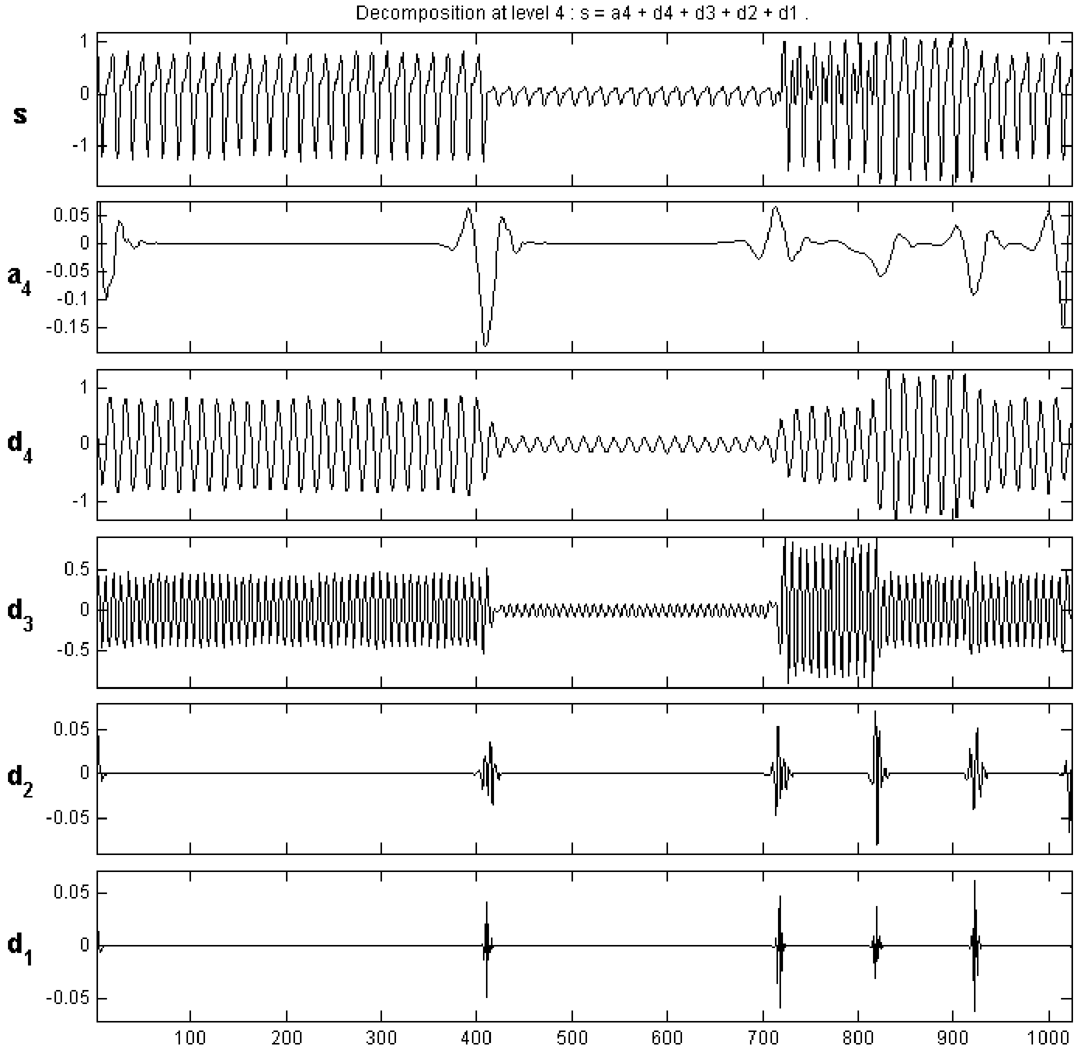

Figure 6.8. DWT decomposition of a EEG signal using db-4 wavelet

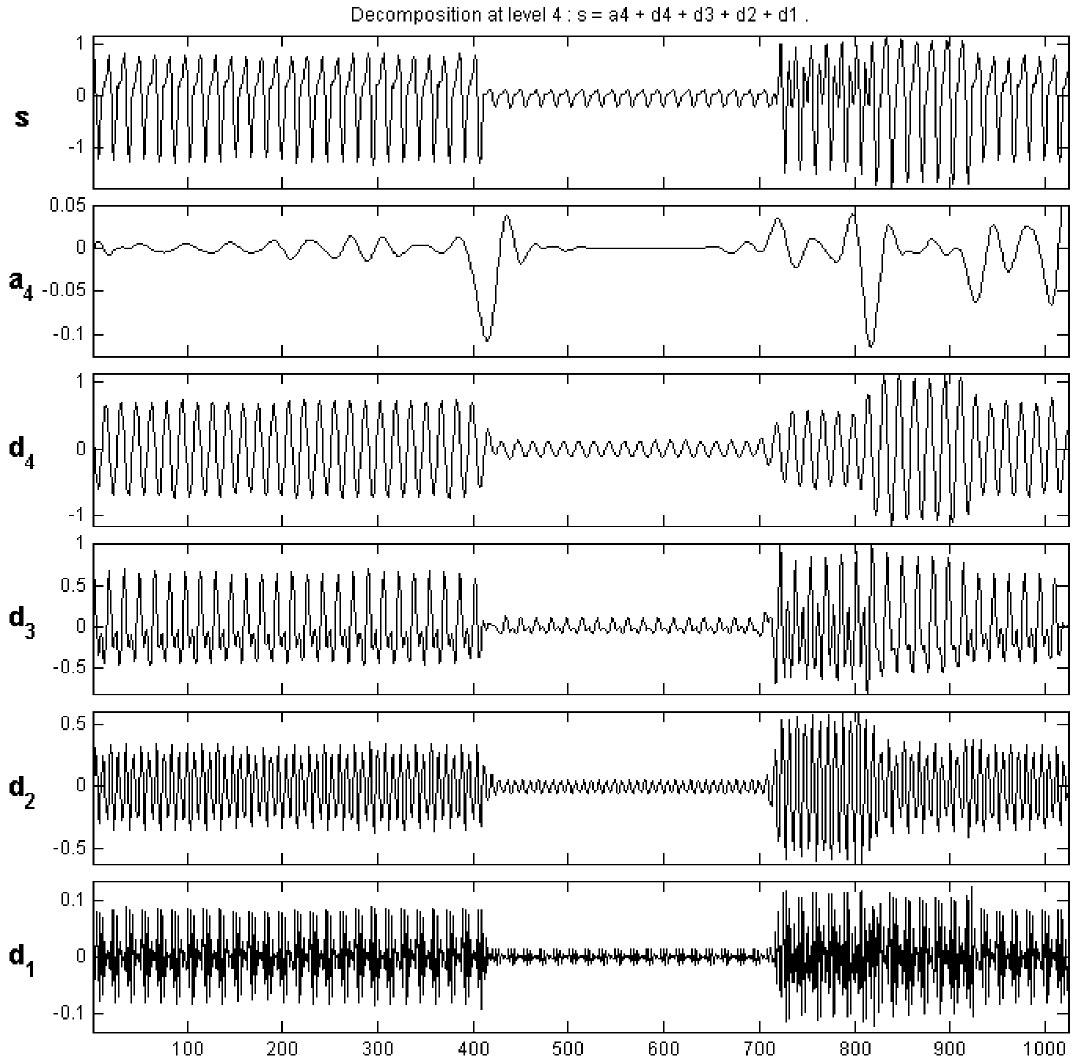

Figure 6.9. DWT decomposition of a EEG signal using db-8 wavelet

The EEG waves can be extracted by decomposition of the data using multilevel discrete wavelet transform (DWT), where DWT contains subband of the signal. Four levels of DWT using EPSP, Meyer, Debauches4 and Debauches8 are implemented. The information about the frequencies of the EEG waves is distributed in several wavelet levels. EPSP functions leads to a better resolution of the event-related oscillations in comparison with a conventional ideal filter used in several previous works. Moreover, due to the fact that the multiresolution decomposition method is implemented as a filtering scheme, it can be seen as a way to construct filters with an optimal time-frequency resolution.

7. CONCLUSION

Wavelet decomposition proved to be a very useful tool for analyzing brain signals. Should be mentioned two advantages of Wavelet transform over Fourier based methods. First, Wavelet Transform lacks of the requirement of stationarity, this being crucial for avoiding spurious results when analyzing brain signals, already known to be highly nonstationary. Second, owing to the varying window size of the Wavelet transform, a better time-frequency resolution can be achieved when the signal has patterns involving different scales. This is particularly important in the case of event-related potentials, where the relevant response is limited to a fraction of a second, a good time resolution thus being crucial for making any physiological interpretation (Suresh and Shankara, 2005).

Scaling and Wavelet functions span approximation and detail spaces correspondingly. These two spaces are complement of each other and their scaled versions constitutes upper or lower spaces. Scaling function is used to approximate the signal (approximation signal) and wavelet function decomposes remaining part (detail) of the signal. Detail of a signal is sometimes refereed as noise. Two band filter banks are discrete correspondence of scaling and wavelet function pairs.

For analysis and approximation of a signal scaling-wavelet function pair which is best to characterize the signal. There are many scaling-wavelet functions defined in literature. An alternative scaling-wavelet function pair is proposed here aimed to analyze bio signals.

Excitory (EPSP) and inhibitory potentials (IPSP) are natural potentials exist at neuron level and if their algebraic sum exceed a threshold the corresponding neuron fires (generate impulse) and measurement of electric potential of a neuron group will is sum of excitory and inhibitory potentials. Since IPSP is negative of EPSP a bio signal can be considered as integral of EPSPs. For this reason EPSP is the basis of a bio signal.

We expect that the future will see the application of the CWT to many of the problems that the DWT has previously been applied to. The often cited argument for using the DWT in an analysis role, because the CWT is significantly more expensive computationally, is most often a spurious one: especially true given the computing power now generally available even in fairly basic medical devices. It will lead to further novel CWT based analysis and compression techniques in the future.

In conclusion, the wavelet transform is a flexible time-frequency decomposition tool which can form the basis of useful signal analysis and coding strategies. An orthogonal scaling-wavelet function pair and their corresponding discrete low pass and high pass filters have been derived from EPSP. They can be used among other scaling-wavelet function pairs to analyze bio signals. It has been shown with EEG signal how the multiresolution decomposition implemented with EPSP functions leads to a better resolution of the event-related oscillations in comparison with a conventional ideal filter used in several previous works. Furthermore, the multiresolution decomposition is a way of data reduction, thus giving relevant coefficients that allows a straightforward implementation of statistical tests. The future will see further application of the wavelet transform to the EEG as the emerging technologies based on them are honed for practical purpose.

REFERENCES

CHAU, F. T., LIANG, Y. Z., GAO, J., SHAO X. G., 2004. Chemometrics From Basics to Wavelet Transform, John Wiley & Sons, Inc., Hoboken, New Jersey.

FLIEGE, N. J., 1996. Multirate Digital Signal Processing (Multirate Systems-Filter Banks-Wavelets). John Wiley & Sons, Chichester, s. 251

FOMITCHEV, M., 1994. An Introduction To Wavelets And Wavelets Transforms. Systems And Programming Inc., Tulsa.

HINRICHS, H., 2004. Electroencephalography, CRC Press LLC.

KAZINNIK, R., ELBER, G., 1997. Orthogonal Decomposition of Non-uniform Bspline Spaces Using Wavelets, Department of Computer Science Technion ITT, volume 16, Israel.

LIEBLING, M., BLU, T., UNSER, M., 2003. Fresnelets: New Multiresolution Wavelet Bases for Digital Holography, IEEE Transactions On Image Processing, Vol. 12, No. 1.

LIN, T., SHI, Q., HAO, P., XU, S., 2003. An Algebraic approach to M-Band Wavelets Construction, National Laboratory on Machine Perception Peking University Beijing, China.

MALLAT, S. A., 1999. Wavelet Tour of Signal Processing, 2nd ed., Academic Pres.

MALLAT, S., 1989. Multiresolution approximations and wavelet orthogonormal bases of $L^2(R)$, Trans. Amer, Math. Soc., 315:69—87.

MERTINS, A., 1999. Signal Analysis: Wavelets, Filter Banks, Time-Frequency Transforms and Applications, John Wiley and Sons Ltd.

POLIKAR, R., GREER, M., UDPA, H. L. and KEINERT, F., 1997. Multiresolution Wavelet Analysis of ERPs for the Detection of Alzheimer's Disease. In Proceedings of the 19th IEEE/EMBS International Conference, volume 30.

PURVES, W. K., ORIANS, G. H., HELLER, H. C. and SADAVA, D., 1998. Life: The Science of Biology (Fifth Edition). Sinauer Associates, Sunderland, MA.

SEMMLOW, J. L., 2004. Biosignal and Biomedical Image Processing Matlab Based Applications, Marcel Dekker, Inc., New York.

STENCEL, J. E., 1992. Using Algorithms in Solving Synapse Transmission Problems: Teaching difficult concepts through a problem-solving approach. Journal of College Science Teaching Sept/Oct:55-57.

STRANG, G. and NGUYEN, T.,1997. Wavelets and Filter Banks, Wellesley-Cambridge Pres, Wellesley, MA.

SURESH, H. N., SHANKARA, V. U., 2005. A New Technique for Multiresolution Characterization of Epileptic Spikes in EEG, Internatıonal Journal Of Informatıon Technology Volume 2 Number 1, ISSN 1305-239X.

TRAN, T. D., R., QUEIROZ, L., NGUYEN, T. Q., 2000. "Linear-Phase Perfect Reconstruction Filter Bank: Lattice Structure, Design, and Application in Image Coding," *IEEE Trans. Signal Proc.*

VETTERLI, M., HERLEY, C., 1992. Wavelets and Filter Banks: Theory and Design. IEEE Trans. Acoust. Speech Signal Process., 40(9):2207-2232.

ZHOU, J., DO, M. N., KOVACCEVIC, J., 2003. New Design of Orthogonal Filter Banks and Wavelets Using the Cayley Transform, IEEE Trans. Signal Proc.

RESUME

Mehmet Kanal was born in Hatay, Turkey in 1980. He received BSc. degree in Electrical - Electronics Engineering Department from Dumlupınar University, Kütahya in 2002. He worked as design engineer at a company is called Tunceroğulları Elektrik & Tuncer Pano in Adana about 2 years. He has been studying for MS degree in Electrical - Electronics Engineering Department of Çukurova University, Adana since 2002. He interested in PC hardware and microcontrollers.

APPENDIX

Matlab Code

```
clear
close all
u = @(t) (1 + sign(t))/2;
c = 6/5; d = 7/5;
n = 7;
to = log(c/d)/(c-d);
phi = @(t) c*d/(d-c)*(exp(-c*t)-exp(-d*t)) .* u(t);
Phi = @(omega) d*c./((i*omega+c).*(i*omega+d));
M = @(omega) d^2*c^2./((omega.^2+c^2).*(omega.^2+d^2));
b = @(omega) M(omega + 5*pi) + M(omega + 4*pi) + M(omega + 2*pi) + ...
    M(omega) + M(omega - 2*pi) + M(omega - 4*pi) + M(omega - 5*pi);

po = zeros(25,1);
for k = -12:12
    f = @(omega) (b(omega)).^(-1/2).*cos(omega*k);
    po(k+13) = 1/pi*quad(f, 0, pi);
end

% Orthogonal phi(t)
phio = @(t) po(1)*phi(t+12) + po(2)*phi(t+11) + po(3)*phi(t+10) + po(4)*phi(t+9)
        + po(5)*phi(t+8) + po(6)*phi(t+7) + po(7)*phi(t+6) + po(8)*phi(t+5) +
          po(9)*phi(t+4) + po(10)*phi(t+3) + po(11)*phi(t+2) + po(12)*phi(t+1) +
          po(13)*phi(t) + po(14)*phi(t-1) + po(15)*phi(t-2) + po(16)*phi(t-3) +
          po(17)*phi(t-4) + po(18)*phi(t-5) + po(19)*phi(t-6) + po(20)*phi(t-7) +
          po(21)*phi(t-8) + po(22)*phi(t-9) + po(23)*phi(t-10) + po(24)*phi(t-11) +
          po(25)*phi(t-12);
```

```
% plot of phi(t) and orthogonal phi(t)
t = linspace(-2, 9, 1000);
figure; plot(t, phi(t)); set(gcf, 'NumberTitle', 'off', 'Name', 'Scaling Function');
axis tight
figure; plot(t, phio(t)); set(gcf, 'NumberTitle', 'off', 'Name', 'Orthogonalized Scaling
Function'); axis tight

% Orthogonal testing
clear t
a = quad(phi, 0, 7);
k = 0;
f = @(t) phi(t).*phi(t-k);
a = quad(f, k, 7);

k = 0;
f = @(t) phio(t).*phio(t-k);
a = quad(f, -2, 9);

% plot of b(w) and b(w)/b(2w)
omega = linspace(-2*pi, 2*pi, 1000);
figure; plot(omega, M(omega)); set(gcf, 'NumberTitle', 'off', 'Name', 'M(omega)');
axis tight
figure; plot(omega, b(omega)); set(gcf, 'NumberTitle', 'off', 'Name', 'b(omega)');
axis tight
figure; plot(omega, b(omega)./b(2*omega)); set(gcf, 'NumberTitle', 'off', 'Name',
'b(omega)/b(2*omega)'); axis tight

% compute lowpass filter coefficients (h(n)
clear omega
m = 12;
p = zeros(2*m+1,1);
```

```
for k = -m:m
    f = @(omega) (b(omega)./b(2*omega)).^(1/2).*cos(omega*k);
    p(k+m+1) = 1/pi*quad(f, 0, pi);
end

clear t omega
n = 12;
a = quad(phi, 0, 7);
y = zeros(n+2, 1);
for k = 0:n-1
   f = @(t) phi(t) .* phi(2*t-k);
   y(k+1) = 2*sqrt(2)*quad(f, 0, 7);
end
y(n+1) = sqrt(2)*a;

b = zeros(n, 1);
for k = 0:n-1
   f = @(t) phi(2*t) .* phi(2*t-k);
   b(k+1) = 4*quad(f, 0, 7);
end

A = [b(1)  b(2)  b(3) b(4) b(5) b(6) b(7) b(8) b(9) b(10) b(11) b(12) 1  1;
      b(2)  b(1)  b(2)  b(3) b(4) b(5) b(6) b(7) b(8) b(9) b(10) b(11) 1  -1;
      b(3)  b(2)  b(1) b(2) b(3) b(4) b(5) b(6) b(7) b(8)  b(9)  b(10) 1  1;
      b(4)  b(3)  b(2)  b(1) b(2) b(3) b(4) b(5) b(6) b(7) b(8)  b(9)  1  -1;
      b(5)  b(4)  b(3) b(2) b(1) b(2) b(3) b(4) b(5) b(6)  b(7)  b(8)  1  1;
      b(6)  b(5)  b(4)  b(3) b(2) b(1) b(2) b(3) b(4) b(5) b(6)  b(7)  1  -1;
      b(7)  b(6)  b(5) b(4) b(3) b(2) b(1) b(2) b(3) b(4)  b(5)  b(6)  1  1;
      b(8)  b(7)  b(6)  b(5) b(4) b(3) b(2) b(1) b(2) b(3) b(4)  b(5)  1  -1;
      b(9)  b(8)  b(7) b(6) b(5) b(4) b(3) b(2) b(1) b(2)  b(3)  b(4)  1  1;
      b(10) b(9)  b(8)  b(7) b(6) b(5) b(4) b(3) b(2) b(1) b(2)  b(3)  1  -1;
```

```
        b(11) b(10) b(9) b(8) b(7) b(6) b(5) b(4) b(3) b(2)  b(1)  b(2)  1  1;
        b(12) b(11) b(10) b(9) b(8) b(7) b(6) b(5) b(4) b(3) b(2)  b(1)  1  -1;
        1     1    1    1    1    1    1    1    1    1     1     1    0  0;
        1    -1    1   -1    1   -1    1   -1    1   -1     1    -1    0   0];
B = inv(A);
h = B*y;
h = h(1:n);

% Orthogonal lowpass filter coefficients
ho = conv(h, p);
kb = floor(m + n/2 -0.5);
ke = ceil(m + n/2 -0.5);
k = (-kb:ke).';

% Orthogonal highpass filter coefficients
go = (-1).^k .* ho((1-k) + ke);

% fine tuning
options = optimset('Display','iter');
[y, fval] = fsolve( @(x) pr(x), ho, options);

figure;
plot((0:35), y, 'r', (0:35), ho, 'b'); axis tight

ho = y;
k = (-kb:ke).';
go = (-1).^k .* ho((1-k) + ke);

% Orthogonal wavelet psio(t)
psio = @(t) go(1)*phio(2*t) + go(2)*phio(2*t-1) + go(3)*phio(2*t-2) +
go(4)*phio(2*t-3) + go(5)*phio(2*t-4) + go(6)*phio(2*t-5) + go(7)*phio(2*t-6) +
```

```
go(8)*phio(2*t-7) + go(9)*phio(2*t-8) + go(10)*phio(2*t-9) + go(11)*phio(2*t-10)+
go(12)*phio(2*t-11) + go(13)*phio(2*t-12) + go(14)*phio(2*t-13) +
go(15)*phio(2*t-14) + go(16)*phio(2*t-15) + go(17)*phio(2*t-16) +
go(18)*phio(2*t-17) + go(19)*phio(2*t-18) + go(20)*phio(2*t-19) +
go(21)*phio(2*t-20) + go(22)*phio(2*t-21) + go(23)*phio(2*t-22) +
go(24)*phio(2*t-23) + go(25)*phio(2*t-24) + go(26)*phio(2*t-25) +
go(27)*phio(2*t-26) + go(28)*phio(2*t-27) + go(29)*phio(2*t-28) +
go(30)*phio(2*t-29) + go(31)*phio(2*t-30) + go(32)*phio(2*t-31) +
go(33)*phio(2*t-32) + go(34)*phio(2*t-33) + go(35)*phio(2*t-34)+
go(36)*phio(2*t-35);

t = linspace(4, 18, 1000);
figure;

plot(t, psio(t)); title('psio(t)'); axis tight

load eeg;
x = eeg;
xa = conv(ho, x); xa = xa(1:2:end);
xb = conv(go, x); xb = xb(1:2:end);
ya = zeros(2*length(xa)-1,1); ya(1:2:end) = xa;
ya = conv(ya, ho(end:-1:1));
yb = zeros(2*length(xb)-1,1); yb(1:2:end) = xb;
yb = conv(yb, go(end:-1:1));
y =  ya + yb;

function y = pr(x)
m = length(x);
n = m/2;
y = zeros(n+1,1);
ytemp = conv(x, x(end:-1:1));
ytemp = ytemp(1:m);
```

```
ytemp = ytemp(2:2:end);
y(1:n) = ytemp;
y(n) = y(n)-1;
y(n+1) = (-1).^(0:m-1) * x;
```